

ALMA MATER STUDIORUM · UNIVERSITÀ DI BOLOGNA

Scuola di Scienze
Dipartimento di Fisica e Astronomia
Corso di Laurea Magistrale in Fisica

A new approach to muon $g-2$ with space-like
data: analysis and fitting procedure.

Relatore:
Prof. Domenico Galli

Presentata da:
Luca Pagani

Correlatori:
Dott. Carlo M. C. Calame
Dott. Umberto Marconi
Dott. Massimo Passera

Anno Accademico 2016/2017

*“Soli omnium otiosi sunt qui sapientiae vacant,
soli vivunt;
nec enim suam tantum aetatem bene tuentur:
omne aevum suo adiciunt: quicquid
annorum ante illos actum est,
illis acquisitum est.”*

*Lucio Anneo Seneca (4a.C.-65d.C.),
De Brevitate Vitae, 14,1.*

Contents

1	The Standard Model prediction of the muon g-2 anomaly	9
1.1	The magnetic moment of the elementary particles.	9
1.2	Muon anomalous magnetic moment	14
1.2.1	The QED contribution to a_μ	15
1.2.2	The electroweak contribution to a_μ	28
1.2.3	The Hadronic contribution to a_μ	30
1.3	Theoretical and experimental value of a_μ	35
1.3.1	The theoretical value of a_μ	36
1.3.2	The experimental value of a_μ	36
1.3.3	Standard Model Vs experiment	39
2	The novel approach to the leading hadronic contribution to muon g-2	41
2.1	μ - e scattering process	43
2.2	Measuring the μ - e elastic differential cross-section.	50
2.3	μ - e fitting process	54
2.4	Computation of the $\Delta\alpha_{had}(t)$ absolute error	59
A	Feynman Parameters	63
A.1	One-loop integrals	63
B	Gordon Identities	65
C	Traces of Dirac matrices	67

Abstract

In the thesis I have studied a new method to measure the Hadronic Leading-Order (HLO) contribution to the muon anomalous magnetic moment a_μ .

In the first part I have described the Standard Model approach to evaluate the muon anomaly. From the perturbative expansion we know that there are many contributions to the muon a_μ : QED contribution, electroweak contribution and hadronic contribution. While the QED and the electroweak contributions to the anomaly can be calculated with increasing precision with the perturbative method, the hadronic contributions at this energy scale cannot, hence experiments are required to estimate its value.

The HLO contribution to the muon anomalous magnetic moment is a vacuum polarization process. It is known since long time that it can be calculated by means of the dispersive approach using $e^- + e^+ \rightarrow \text{hadrons}$ s-channel, time-like, annihilation data. I have studied the dispersive method, based on the optical theorem and dispersion relations, in all the details.

Subsequently I have discussed why this method could hardly further improve the theoretical uncertainty. Dominant contributions to the dispersive integral are due to the well-known hadronic resonant contributions, with $\sqrt{s} < 2$ GeV. Moreover with the additional complication that one has to evaluate all the contributions, due to different hadronic final states, that must be taken from many different experiments.

In the second part of the thesis I studied an innovative proposal to measure the HLO contribution to a_μ . The novel method is based on the idea of using the elastic scattering of high energetic muons on at rest electrons $\mu + e^- (\text{rest}) \rightarrow \mu + e^-$. The strength of the idea is to rely on t-channel scattering data, with four-momentum transfer $t = q^2 < 0$ in space-like region to measure the HLO to a_μ . In this case the differential elastic cross-section allows to measure the running of $\alpha(t)$ with very high precision and to determine the hadronic shift $\Delta\alpha_{had}(t)$ subtracting all the contributions due to QED and electroweak processes to the relevant perturbative order. Through $\Delta\alpha_{had}(t)$ the HLO contribution to a_μ can be calculated integrating a smooth function, of the transferred momentum, exploiting just a single scattering process.

I have performed a preliminary study of the fitting procedure to extract $\Delta\alpha_{had}(t)$ from the cross-section. At this stage I used a sample of data obtained using the Leading-Order approximation of the scattering cross-section. I have studied the systematics effects

affecting the fit as a function of the interpolating function models. According to the present estimates this new approach, which represents an independent complementary technique to evaluate the HLO corrections to a_μ , will reach a precision competitive with the precision of the present results, of the level or even better than 0.6%, in just two years of data taking.

Notations and Conventions

Tensor

The conventions used in the thesis follow Jackson (1975), Bjorken and Drell (1964) conventions. The metric tensor is:

$$g_{\mu\nu} = g^{\mu\nu} = \begin{pmatrix} 1 & 0 & 0 & 0 \\ 0 & -1 & 0 & 0 \\ 0 & 0 & -1 & 0 \\ 0 & 0 & 0 & -1 \end{pmatrix}$$

with Greek indices running over 0,1,2,3. Roman indices denote only the three spatial components. Repeated indices are summed in all cases. Four-vectors are denoted by light italic type, three-vectors are denoted by boldface type.

Relativity

The following notation denotes a space-time point:

$$x^\mu = (x^0, \mathbf{x}), \quad x_\mu = g_{\mu\nu} x^\nu = (x^0, -\mathbf{x})$$

the displacement of x^μ is “naturally raised”, while the derivative operator

$$\partial_\mu \frac{\partial}{\partial x^\mu} = \left(\frac{\partial}{\partial x^0}, \nabla \right)$$

is “naturally lowered”.

For a massive particle:

$$p^2 = p_\mu p^\mu = E^2 - |\mathbf{p}|^2 = m^2$$

Quantum Mechanics

The energy and momentum operators acting on a wave function as:

$$E = i \frac{\partial}{\partial x^0}, \quad \mathbf{p} = -i \nabla$$

in compact notation

$$p^\mu = i \partial^\mu$$

The Pauli spin matrices are three Hermitean 2×2 matrices

$$\sigma_1 = \begin{pmatrix} 0 & 1 \\ 1 & 0 \end{pmatrix}, \quad \sigma_2 = \begin{pmatrix} 0 & -i \\ i & 0 \end{pmatrix}, \quad \sigma_3 = \begin{pmatrix} 1 & 0 \\ 0 & -1 \end{pmatrix}$$

which satisfy

$$\sigma_i \sigma_j = \delta_{ij} + i \varepsilon_{ijk} \sigma_k$$

where $\varepsilon_{123} = \varepsilon^{123} = 1$ so that

$$\{\sigma_i, \sigma_j\} = 2\delta_{ij}, \quad [\sigma_i, \sigma_j] = 2i\varepsilon_{ijk} \sigma_k$$

Dirac matrices

The Dirac matrices in the Weyl, or spinorial, or even chiral representation are

$$\gamma^0 = \begin{pmatrix} 0 & \mathbf{1} \\ \mathbf{1} & 0 \end{pmatrix} \quad \gamma^i = \begin{pmatrix} 0 & \sigma_i \\ -\sigma_i & 0 \end{pmatrix}$$

they satisfy the following Clifford algebra

$$\{\gamma^\mu; \gamma^\nu\} = 2g^{\mu\nu} \mathbb{1}$$

while the commutator is defined as

$$\sigma^{\mu\nu} \equiv \frac{i}{4} [\gamma^\mu; \gamma^\nu]$$

The Dirac's matrices satisfy the following Hermitian property

$$\gamma^{\mu\dagger} = \gamma^0 \gamma^\mu \gamma^0$$

so that

$$\beta = \gamma^0 = \begin{pmatrix} 0 & \mathbf{1} \\ \mathbf{1} & 0 \end{pmatrix} \quad \alpha^i = \begin{pmatrix} -\sigma^i & 0 \\ 0 & \sigma^i \end{pmatrix}$$

Finally

$$\gamma_5 = \gamma^5 = \begin{pmatrix} -\mathbf{1} & 0 \\ 0 & \mathbf{1} \end{pmatrix} \tag{1}$$

We always use the Weyl representation of Dirac's matrices, unless it is specified.

Chapter 1

The Standard Model prediction of the muon g-2 anomaly

The Standard Model (SM) prediction of the muon anomalous magnetic moment has occupied many physicists for over 70 years: from the P. Dirac's prediction (1928) and J. Schwinger's calculation (1948) of QED one-loop correction, until the last accurate calculation of higher-order QED corrections of S. Laporta (2017). Nowadays, the discussion about its theoretical value is still open.

1.1 The magnetic moment of the elementary particles.

Classical electrodynamics predicts that a rotating electrically charged body creates a *magnetic dipole moment*. According to Quantum Mechanics, due to its spin (the particle intrinsic angular momentum), it follows that each charged particle has a magnetic dipole moment.

Let's consider for instance the case of the electron, whose mass is m_e and its charge is set to $-e$, moving with velocity of magnitude v in a circular Bohr orbit of radius r . The charge circulating in a loop (the electron's orbit) is equivalent to a current:

$$i = -\frac{e}{T} = -\frac{ev}{2\pi r} \quad (1.1)$$

where T is the orbital period of the electron. Relying on classical electromagnetism, it can be shown that such a current loop produces a magnetic dipole moment. For a given current of intensity i , circulating in a loop of area A , the magnitude of the orbital magnetic dipole moment μ_l is

$$\mu_l = iA \quad (1.2)$$

Since the electron has a negative charge its magnetic dipole moment μ_l is anti-parallel to its orbital angular momentum \mathbf{L} , whose magnitude is given by:

$$L = m_e v r \quad (1.3)$$

Evaluating i from equation (1.1) and A for a circular Bohr orbit from (1.2), we obtain:

$$\mu_l = iA = -\frac{evr}{2} \quad (1.4)$$

dividing by angular momentum (1.3), it yields:

$$\frac{\mu_l}{L} = -\frac{e}{2m_e} \quad (1.5)$$

Therefore, the ratio of the electron magnetic moment and electron angular momentum is a combination of universal constants. It is usual to write this ratio as

$$\frac{\mu_l}{L} = -\frac{g_l \mu_B}{\hbar} \quad (1.6)$$

where μ_B is called Bohr magneton, its value, in the International System of unit, is:

$$\mu_B = e\hbar/(2m_e) = 9.27400949(80) \times 10^{-24} \text{J} \cdot \text{T}^{-1} \quad (1.7)$$

where the coefficient g_l , called *orbital g-factor* (or more correctly *Landé g-factor*), is equal to:

$$g_l = 1 \quad (1.8)$$

Rewriting the equation (1.6) in vector notation we get:

$$\boldsymbol{\mu}_l = -\frac{g_l \mu_B}{\hbar} \mathbf{L} = -\frac{g_l e}{2m_e} \mathbf{L} \quad (1.9)$$

It is possible to show that the previous formula is completely independent of the details of the orbit.

In Quantum Mechanics the angular momentum has a discrete spectrum of eigenvalues, i.e. it takes the values $L = \sqrt{l(l+1)}\hbar$, so that the electron magnetic moment is:

$$\mu_l = -\frac{g_l \mu_B}{\hbar} L = -g_l \mu_B \sqrt{l(l+1)} \quad (1.10)$$

with projection:

$$\mu_{l_z} = -\frac{g_l \mu_B}{\hbar} L_z = -g_l \mu_B m_l \quad (1.11)$$

the crucial result, we get with the last formula, is the discretely quantized values of μ_{l_z} , with m_l

$$m_l = -l, -l+1, \dots, 0, \dots, +l-1, +l$$

Thus, according to eq. (1.11) the number of possible values of μ_{l_z} is equal to $2l+1$. Experiments, by Stern and Gerlach experiment (1922), and the Philips and Taylor experiment (1927), proved that eq. (1.11) holds, with the number of possible projections m_l equal to two. This result implies that electron has an intrinsic magnetic moment μ_s ,

related to its intrinsic spin angular momentum \mathbf{S} . Similarly to the previous case of the orbital angular momentum L , for the spin we have

$$S = \sqrt{s(s+1)}\hbar \quad (1.12)$$

$$S_z = m_s \hbar \quad (1.13)$$

The relation between the spin magnetic dipole moment and the spin angular momentum is then the same as the relation for the orbital case:

$$\boldsymbol{\mu}_s = -\frac{g_s \mu_B}{\hbar} \mathbf{S} \quad (1.14)$$

$$\mu_{s_z} = -g_s \mu_B m_s \quad (1.15)$$

where the quantity g_s is called *spin g-factor*.

It is an experimental fact that μ_{s_z} can assume just two values, which are equal in magnitude but opposite in sign [1]. In the assumption that the possible values of m_s are in range from $-s$ to $+s$ it is possible to conclude that:

$$m_s = -1/2, +1/2 \quad (1.16)$$

and that s has a single value

$$s = 1/2 \quad (1.17)$$

In the two experiments it was possible to determine that $g_s m_s = \pm 1$ [2]. Since we have already established that $m_s = -1/2, +1/2$, it implies

$$g_s = 2 \quad (1.18)$$

The theoretical explanation of the last result was given by Dirac. It follows directly from the relativistic wave equation for the $1/2$ spin electrons. In order to prove this statement, we will make use of Dirac matrices in the Dirac representation:

$$\gamma_D^0 = \begin{pmatrix} -i & 0 \\ 0 & i \end{pmatrix} \quad \beta_D = \begin{pmatrix} \mathbf{1} & 0 \\ 0 & -\mathbf{1} \end{pmatrix} \quad \alpha_D^i = \begin{pmatrix} 0 & \sigma^i \\ \sigma^i & 0 \end{pmatrix} \quad (1.19)$$

Let's consider first the Dirac equation in the Hamiltonian form:

$$i\hbar \partial_t \psi(t, \mathbf{x}) = H_D \psi(t, \mathbf{x}) \quad (1.20)$$

where H_D is the Dirac's Hamiltonian:

$$H_D = c\mathbf{p} \cdot \boldsymbol{\alpha}_D + m_e c^2 \beta_D \quad (1.21)$$

We are interested in studying the interaction of the electron with the external electromagnetic field:

$$A^\mu(t, \mathbf{x}) = (\phi(t, \mathbf{x}), \mathbf{A}(t, \mathbf{x})) \quad (1.22)$$

The interaction of the electron with the electromagnetic field can be described by means of the minimal coupling

$$H_D \rightarrow H_D - e\phi \quad \mathbf{p} \rightarrow \mathbf{p} - \frac{e}{c}\mathbf{A} \equiv \boldsymbol{\pi} \quad (1.23)$$

in this way, eq. (1.21) reads

$$H_D = c\boldsymbol{\pi} \cdot \boldsymbol{\alpha}_D + m_e c^2 \beta_D + e\phi \quad (1.24)$$

Now, replacing the Hamiltonian of eq. (1.20) with eq. (1.24), we obtain

$$i\hbar\partial_t\psi(t, \mathbf{x}) = (c\boldsymbol{\pi} \cdot \boldsymbol{\alpha}_D + m_e c^2 \beta_D + e\phi) \psi(t, \mathbf{x}) \quad (1.25)$$

taking into account that we are working in the non-relativistic limit, we can rewrite the wave function as

$$\psi(t, \mathbf{x}) = e^{-i/\hbar m_e c^2 t} \begin{pmatrix} \varphi(t, \mathbf{x}) \\ \chi(t, \mathbf{x}) \end{pmatrix} \quad (1.26)$$

namely, factoring the temporal part, which presence is due to the energy connected to the electron mass, and splitting the Dirac spinor into two components spinors φ and χ . Replacing the spinor of eq. (1.25) with eq. (1.26), it is easy to obtain

$$i\hbar\partial_t\varphi = c\boldsymbol{\sigma} \cdot \boldsymbol{\pi} + e\phi\varphi \quad (1.27a)$$

$$m_e c^2 \chi + i\partial_t\chi = c\boldsymbol{\sigma} \cdot \boldsymbol{\pi}\varphi - m_e c^2 \chi + e\phi\chi \quad (1.27b)$$

on the left side of eq. (1.27b) it is possible to ignore the term with temporal dependence, on the right side the term with the electrical potential. We can apply these simplifications because both terms are negligible compared to the massive term. In other words, we can neglect the terms that are small when $c \rightarrow \infty$.

Solving eq. (1.27b)

$$\chi = \frac{\boldsymbol{\sigma} \cdot \boldsymbol{\pi}}{2m_e c} \varphi \quad (1.28)$$

and substituting in eq. (1.27a), we get

$$i\hbar\partial_t\varphi = \left(\frac{(\boldsymbol{\sigma} \cdot \boldsymbol{\pi})^2}{2m_e} + e\phi \right) \varphi \quad (1.29)$$

Making use of the algebra of the Pauli matrices

$$\begin{aligned}
(\boldsymbol{\sigma} \cdot \boldsymbol{\pi})^2 &= \pi^i \pi^j \sigma^i \sigma^j \\
&= \pi^2 + i\varepsilon^{ijk} \pi^i \pi^j \sigma^k \\
&= \pi^2 + i\varepsilon^{ijk} \frac{1}{2} [\pi^i, \pi^j] \sigma^k \\
&= \pi^2 + i\varepsilon^{ijk} \frac{i\hbar e}{2c} (\partial^i A^j - \partial^j A^i) \sigma^k \\
&= \pi^2 - \frac{\hbar e}{2c} \varepsilon^{ijk} \varepsilon_{ijl} B^l \sigma^k \\
&= \pi^2 - \frac{\hbar e}{2c} 2\delta^{kl} B^l \sigma^k \\
&= \pi^2 - \frac{\hbar e}{c} B^k \sigma^k
\end{aligned} \tag{1.30}$$

and, furthermore, defining the spin operator as $\mathbf{S} = \frac{1}{2}\hbar\boldsymbol{\sigma}$, we obtain

$$(\boldsymbol{\sigma} \cdot \boldsymbol{\pi})^2 = \pi^2 - \frac{2e}{c} \mathbf{S} \cdot \mathbf{B} \tag{1.31}$$

Now, the eq. (1.29) reads

$$i\hbar\partial_t\varphi = \left(\frac{\pi^2}{2m_e} - \frac{e}{m_e c} \mathbf{S} \cdot \mathbf{B} + e\phi \right) \varphi \tag{1.32}$$

usually known as *Pauli equation*.

By comparing the second term on the right side of Pauli equation with eq. (1.14), we finally obtain the expected result:

$$g_s = 2 \tag{1.33}$$

However, after a long experimental effort it was finally possible to prove that the measured value of g_s disagree with the Dirac's predicted one.

As a matter of fact, the experimental value of electron g_s , with remarkable precision is currently established to be [3]:

$$g_s^{exp} = (20023193043618.2 \pm 5.2) \times 10^{-13} \tag{1.34}$$

The experimental value is slightly larger than the Dirac's predicted value, at the level of 0.1%. This small correction is known as the *anomalous magnetic dipole moment* of the electron. According to Quantum Electrodynamics (QED) the anomaly arises from the electron interactions with the virtual photons, that are off-shell quanta of the electromagnetic field.

It is common practice to express the anomalous magnetic moment of electron as:

$$a_e = \frac{\mu_e}{\mu_B} - 1 = \frac{g_s - 2}{2} \quad (1.35)$$

or in the almost widespread form as electron $g-2$, which is correctly named dimensionless anomalous magnetic moment.

Nowadays, the electron $g - 2$ is still not a failure of theory. On the contrary, it represents the strongest demonstration of the predicting power of the Standard Model. The theoretical and the experimental value of electron anomalous magnetic moment agree up to the twelfth significant digit.

Of course the electrons were not the only particles known before the development of Standard Model theoretical structure. For instance physicists had discovered nucleons (protons and neutrons), even if for some time they may have thought these were elementary particles. Instead nucleons have an anomalous magnetic moments that cannot be explained assuming a point like structure, as it is for the electron. The explanation of protons and neutrons anomalous magnetic moment came in fact much recently with the introduction of the quarks theory by Gell-Mann, because of the magnetic moment of the nucleons can be modeled as a sum of the magnetic moments of the constituent quarks.

1.2 Muon anomalous magnetic moment

The eventual recognition of the muon as a "heavy electron" brought up the question if it could have been considered a point-like particle. The muon, as the electron, has an anomalous magnetic moment, known as muon ($g - 2$), or a_μ .

In this thesis, we get the following value for the muon anomalous magnetic moment:

$$a_\mu^{SM} = (11659175.7 \pm 5.7) \times 10^{-10} \quad [0.5 \text{ ppm}] \quad (1.36)$$

according to the most accurate theoretical results of QED and electroweak contributions and to lasts F. Jegerlehner results of the hadronic leading-order and higher-order corrections [48].

The theoretical value of muon $g - 2$ is obtained, according to quantum field theory, computing each Feynman diagram, which is the perturbative correction to the tree-level diagram, shown in figure 1.1, and cutting off the perturbative series at desired order.

To obtain this value is necessary to distinguish the three different contributions that are involved in the perturbative series: QED contribution, electroweak contribution and hadronic contribution. Thus we can write

$$a_\mu^{SM} = a_\mu^{QED} + a_\mu^{EW} + a_\mu^{had} \quad (1.37)$$

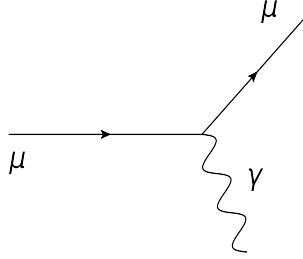


Figure 1.1: Muon tree-level diagram.

1.2.1 The QED contribution to a_μ

The QED contribution to the anomalous magnetic moment of the muon is defined as the contribution arising from the subset of SM diagrams containing only leptons (e , μ , τ) and photons (γ). The QED contribution to a_μ can be evaluated, as a dimensionless quantity, by the perturbative expansion in α/π [4]

$$\begin{aligned} a_\mu^{QED} &= \sum_{n=1}^{\infty} \left(\frac{\alpha}{\pi}\right)^n C_n \\ &= \left(\frac{\alpha}{\pi}\right) C_1 + \left(\frac{\alpha}{\pi}\right)^2 C_2 + \left(\frac{\alpha}{\pi}\right)^3 C_3 + \left(\frac{\alpha}{\pi}\right)^4 C_4 + \left(\frac{\alpha}{\pi}\right)^5 C_5 + \dots \end{aligned} \quad (1.38)$$

where C_n is finite, thanks to the renormalizability of QED, and it can be computed order-by-order. It can be split in

$$C_n = A_1^{(2n)} + A_2^{(2n)}(m_\mu/m_e) + A_2^{(2n)}(m_\mu/m_\tau) + A_3^{(2n)}(m_\mu/m_e, m_\mu/m_\tau) \quad (1.39)$$

where m_e , m_μ , m_τ are the masses of the electron, muon and tau, respectively. The term A_1 is mass independent because it arises from diagrams containing only photons and muons. Due to this mass independence, A_1 turns out to be an universal term: it is the same for all the anomalous magnetic moment of the three leptons. On the contrary, A_2 and A_3 are mass dependent, because they are generated by graphs containing also electrons and taus.

C_1 : the one-loop contribution

Only one diagram, shown in figure 1.2, carries one-loop. The result of this diagram was calculated by Schwinger, and it was the first great theoretical achievement of QED. The outcome of the computation is graven on Schwinger's tomb.

Applying Feynman rules on figure 1.2 for an incoming muon of four-momentum p^ν , a photon of four-momentum k^ν , an outgoing muon of four-momentum q^ν and a virtual photon of four-momentum l^ν , we have:

$$\bar{u}(q)\Gamma^\mu(p, q)u(p) = \int \frac{d^4l}{(2\pi)^4} \bar{u}(q) (-ie\gamma^\rho) S(p+l) \gamma^\mu S(q+l) (-ie\gamma^\sigma) D_{\rho\sigma}(l)u(p) \quad (1.40)$$

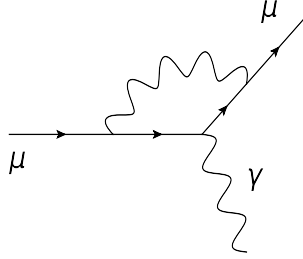


Figure 1.2: One-loop QED correction diagram.

where the four-momentum conservation brings to $p + k = q$. The photon propagator $D_{\rho\sigma}(l)$ and the muon propagator $S(p + l)$ are as usual:

$$D_{\rho\sigma}(l) = \frac{-ig_{\rho\sigma}}{l^2 + i\varepsilon} \quad S(p + l) = \frac{i(\not{l} + \not{p} + m_\mu)}{(l + p)^2 - m_\mu^2 + i\varepsilon}$$

The calculation procedure we will use is quite different from the standard derivation of the Schwinger's result, but it is more general. Indeed for solving this integral the Pauli-Villars regularization is enough [5], but we prefer to proceed making use of the dimensional regularization [6].

Setting $\epsilon = 2 - \omega$, it is possible to write:

$$\begin{aligned} \Gamma^\mu(p, q) &\doteq \frac{e^2 \mu^{2\epsilon}}{i(2\pi)^{2\omega}} \int d^{2\omega} l \frac{[\gamma^\rho(\not{l} + \not{p} + m_\mu)\gamma^\mu(\not{l} + \not{q} + m_\mu)\gamma_\rho]}{[(l + p)^2 - m_\mu^2 + i\varepsilon][(l + q)^2 - m_\mu^2 + i\varepsilon](l^2 + i\varepsilon)} \\ &\equiv \frac{e^2 \mu^{2\epsilon}}{i(2\pi)^{2\omega}} \int d^{2\omega} l \frac{N(l, p, q)}{D(l, p, q)} \end{aligned} \quad (1.41)$$

with the arbitrary mass scale μ , introduced with a suitable exponent, in such a manner to deal with a dimensionless of the integral. The symbol \doteq means that spin states $\bar{u}(q)(\dots)u(p)$, the Dirac equation and the mass-shell condition are tacitly understood.

Feynman's parametric rule must be used to simplify the denominator [7]:

$$\frac{1}{AB^n} = \int_0^1 dx \int_0^1 dy \delta(1 - x - y) \frac{ny^{n-1}}{[xA + yB]^{n+1}} \quad (1.42)$$

in the particular case of eq. (1.41), Feynman's rule reads:

$$\begin{aligned}
\frac{1}{ABC} &= \frac{1}{C} \int_0^1 dx \int_0^1 dy \delta(1-x-y) [xA + yB]^{-2} \\
&= \frac{1}{C} \int_0^1 dx [xA + (1-x)B]^{-2} \\
&= \int_0^1 dx \int_0^1 dy \int_0^1 dz \delta(1-y-z) 2y [xyA + (1-x)yB + zC]^{-3} \\
&= \int_0^1 dx \int_0^1 dy 2y [xyA + (1-x)yB + (1-y)C]^{-3}
\end{aligned} \tag{1.43}$$

It is also useful to apply the following change of variable

$$\begin{aligned}
x &\equiv v(1-u)^{-1} & y &\equiv 1-u \\
\left| \frac{\partial(x,y)}{\partial(u,v)} \right| &= \frac{1}{1-u}
\end{aligned} \tag{1.44}$$

with $0 \leq u \leq 1$ and $0 \leq v \leq 1-u$. Under this change, eq. (1.43) reads:

$$\frac{1}{ABC} = \int_0^1 du \int_0^{1-u} dv \frac{2}{[vA + (1-u-v)B + uC]^3} \tag{1.45}$$

It follows that the denominator $D(l, p, q)$ of eq. (1.41) becomes:

$$\begin{aligned}
\frac{1}{D(l, p, q)} &= \int_0^1 du \int_0^{1-u} dv \frac{2}{D^3(l, p, q, u, v)} \\
&= \int_0^1 du \int_0^{1-u} dv \\
&\quad \times \frac{2}{[v[(l+q)^2 - m_\mu^2 + i\varepsilon] + (1-u-v)(l^2 + i\varepsilon) + u[(l+p)^2 - m_\mu^2 + i\varepsilon]]^3} \\
&= \int_0^1 du \int_0^{1-u} dv \frac{2}{[l^2 + 2l(qv + pu) - m_\mu^2(v+u) + vq^2 + up^2 + i\varepsilon]^3}
\end{aligned} \tag{1.46}$$

To further simplify $D(l, p, q, u, v)$ we have to operate the translation:

$$l \rightarrow l - up - vq \tag{1.47}$$

which reduces the denominator of eq. (1.46) to:

$$D(l, p, q, u, v) = l^2 - m_\mu^2(u+v) + up^2(1-u) + vq^2(1-v) - 2upvq + i\varepsilon \tag{1.48}$$

Now we must apply the same translation into the numerator:

$$N(l, p, q) \rightarrow N(l, p, q, u, v)$$

making clear

$$\begin{aligned} N(l, p, q, u, v) &= [\gamma^\rho (\not{l} - u\not{p} - v\not{q} + \not{p} + m_\mu) \gamma^\mu (\not{l} - u\not{p} - v\not{q} + \not{q} + m_\mu) \gamma_\rho] \\ &= \gamma^\rho [\not{l} + \not{p}(1-u) - v\not{q}] \gamma^\mu [\not{l} + \not{q}(1-v) - u\not{p}] \gamma_\rho \\ &\quad + m_\mu \{ \gamma^\rho [\not{p}(1-u) - v\not{q}] \gamma^\mu \gamma_\rho + \gamma^\rho \gamma^\mu [\not{q}(1-v) - u\not{p}] \gamma_\rho \} \\ &\quad + m_\mu^2 \gamma^\rho \gamma^\mu \gamma_\rho + \text{irrelevant} \end{aligned}$$

where *irrelevant* stands for terms linear in l^μ , that vanish owing to symmetric integration. Since the denominator of eq. (1.48) depends only on the magnitude of l^μ , one obtain:

$$\int \frac{d^{2\omega}}{(2\pi)^{2\omega}} \frac{l^\mu}{D^3(l, p, q, u, v)} = 0 \quad (1.49)$$

Collecting together all these results, we have:

$$\Gamma^\mu(p, q) \doteq \Gamma_{div}^\mu(p, q) + \Gamma_{fin}^\mu(p, q) \quad (1.50)$$

where

$$\begin{aligned} \Gamma_{div}^\mu(p, q) &\doteq \frac{2e^2 \mu^{2\epsilon}}{i(2\pi)^{2\omega}} \int_0^1 du \int_0^{1-u} dv \gamma^\rho \gamma^\alpha \gamma^\mu \gamma^\beta \gamma_\rho \\ &\quad \times \int d^{2\omega} l \frac{l_\alpha l_\beta}{[l^2 - m_\mu^2(u+v) + up^2(1-u) + vq^2(1-v) - 2uvp \cdot q + i\varepsilon]^3} \\ \Gamma_{fin}^\mu(p, q) &\doteq \frac{2e^2}{i(2\pi)^2} \int_0^1 du \int_0^{1-u} dv \gamma^\rho [(1-u)\not{p} - v\not{q} + m_\mu] \gamma^\mu [(1-v)\not{q} - u\not{p} + m_\mu] \gamma_\rho \\ &\quad \times \int d^4 l \frac{1}{[l^2 - m_\mu^2(u+v) + up^2(1-u) + vq^2(1-v) - 2uvp \cdot q + i\varepsilon]^3} \end{aligned} \quad (1.51)$$

Only $\Gamma_{div}^\mu(p, q)$ contains the divergent part of the Feynman integral, on the contrary $\Gamma_{fin}^\mu(p, q)$ represents a convergent integral, therefore we can set, for it, $\omega = 2$.

Making use of basic one-loop Feynman integrals (eqq. A.2 and A.3) to solve the integration in the l variable, we get:

$$\begin{aligned} \Gamma_{div}^\mu(p, q) &\doteq \frac{\alpha}{8\pi} (4\pi\mu^{2-\omega}) \Gamma(2-\omega) \\ &\quad \times \int_0^1 \int_0^{1-u} \frac{\gamma^\rho \gamma^\alpha \gamma^\mu \gamma_\alpha \gamma_\rho}{[(u+v)m_\mu^2 + 2uvp \cdot q - u(1-u)p^2 - v(1-v)q^2]^{2-\omega}} \\ \Gamma_{fin}^\mu(p, q) &\doteq \frac{(-\alpha)}{4\pi} \int_0^1 du \int_0^{1-u} dv \frac{\gamma^\rho [(1-u)\not{p} - v\not{q} + m_\mu] \gamma^\mu [(1-v)\not{q} - u\not{p} + m_\mu] \gamma_\rho}{u(1-u)p^2 + v(1-v)q^2 - (u+v)m_\mu^2 - 2uvp \cdot q} \end{aligned} \quad (1.52)$$

To recast the numerator of the former fraction in a simple form, the following identities in a space with 2ω -dimension are useful:

$$\gamma^\mu \gamma_\mu = 2\omega \mathbb{1}_{2\omega} \quad (1.53a)$$

$$\gamma^\mu \gamma^\nu \gamma_\mu = (2 - 2\omega) \gamma^\nu \quad (1.53b)$$

$$\gamma^\mu \gamma^\nu \gamma^\rho \gamma_\mu = 4g^{\nu\rho} \mathbb{1}_{2\omega} - (4 - 2\omega) \gamma^\nu \gamma^\rho \quad (1.53c)$$

$$\gamma^\mu \gamma^\nu \gamma^\rho \gamma^\sigma \gamma_\mu = (4 - 2\omega) \gamma^\nu \gamma^\rho \gamma^\sigma - 2\gamma^\sigma \gamma^\rho \gamma^\nu \quad (1.53d)$$

Using eqq. (1.53a)-(1.53a), we can write:

$$\begin{aligned} \Gamma_{div}^\mu(p, q) &\doteq \Gamma(2 - \omega) \gamma^\mu \frac{\alpha}{2\pi} (1 - \omega)^2 (4\pi\mu^2)^{2-\omega} \\ &\quad \times \int_0^1 du \int_0^{1-u} dv [m_\mu^2(u+v) + 2uvp \cdot q - u(1-u)p^2 - v(1-v)q^2]^{\omega-2} \\ &\doteq \left(\frac{1}{\epsilon} - \mathbf{C} + \dots \right) \gamma^\mu \frac{\alpha}{2\pi} (\epsilon - 1)^2 \\ &\quad \times \int_0^1 du \int_0^{1-u} dv \left[\frac{m_\mu^2(u+v) + 2uvp \cdot q - u(1-u)p^2 - v(1-v)q^2}{4\pi\mu^2} \right]^{-\epsilon} \\ &\doteq \gamma^\mu \frac{\alpha}{4\pi} \left(\frac{1}{\epsilon} - \mathbf{C} - 2 \right) \\ &\quad - 2\gamma^\mu \frac{\alpha}{4\pi} \int_0^1 \int_0^{1-u} dv \ln \left(\frac{m_\mu^2(u+v) + 2uvp \cdot q - u(1-u)p^2 - v(1-v)q^2}{4\pi\mu^2} \right) \end{aligned} \quad (1.54)$$

the result is obtained up to evanescent terms for $2 - \omega = \epsilon \rightarrow 0$. Therefore, we find:

$$\Gamma_{div}^\mu(p, q) \doteq \gamma^\mu \left[\frac{\alpha}{4\pi} \frac{1}{\epsilon} + \text{finite part} \right] \quad (1.55)$$

Now it is necessary to evaluate the above ultraviolet divergent term on the particle

mass-shell $p^2 = q^2 = m_\mu^2$ with $k = q - p$ and $k^2 = 0$. We find:

$$\begin{aligned}
\Gamma_{div}^\mu &\doteq \gamma^\mu \frac{\alpha}{4\pi} \left(\frac{1}{\epsilon} - \mathbf{C} - 2 \right) \\
&\quad - 2\gamma^\mu \frac{\alpha}{4\pi} \int_0^1 \int_0^{1-u} dv \ln \left(\frac{m_\mu^2(u+v) + 2uvp(p+k) - u(1-u)p^2 - v(1-v)q^2}{4\pi\mu^2} \right) \\
&\doteq \gamma^\mu \frac{\alpha}{4\pi} \left(\frac{1}{\epsilon} - \mathbf{C} - 2 \right) \\
&\quad - 2\gamma^\mu \frac{\alpha}{4\pi} \int_0^1 \int_0^{1-u} dv \ln \left(\frac{m_\mu^2(u+v) + 2uvm_\mu^2 - u(1-u)m_\mu^2 - v(1-v)m_\mu^2}{4\pi\mu^2} \right) \\
&\doteq \gamma^\mu \frac{\alpha}{4\pi} \left\{ \frac{1}{\epsilon} - \mathbf{C} - 2 + 2 \int_0^1 \int_0^{1-u} dv \ln \frac{4\pi\mu^2}{m_\mu^2} - 2 \ln(u+v) \right\}
\end{aligned} \tag{1.56}$$

in which the following relation has been used:

$$p + k = q \rightarrow (q - p)^2 = k^2 \rightarrow q^2 + p^2 - 2pq = 0 \rightarrow pq = m_\mu^2$$

Continuing in the computation, solving the integrals:

$$\begin{aligned}
\Gamma_{div}^\mu &\doteq \gamma^\mu \frac{\alpha}{4\pi} \left\{ \frac{1}{\epsilon} - \mathbf{C} - 2 + 2 \int_0^1 du \left[(1-u) \ln \left(\frac{4\pi\mu^2}{m_\mu^2} \right) + 2(1-u + u \ln u) \right] \right\} \\
&\doteq \gamma^\mu \frac{\alpha}{4\pi} \left\{ \frac{1}{\epsilon} - \mathbf{C} - 1 + \ln \left(\frac{4\pi\mu^2}{m_\mu^2} \right) \right\}
\end{aligned} \tag{1.57}$$

thus the divergence has been removed and the integral has been calculated.

Now we have to solve the finite integral of eq. (1.51). To this purpose turns out to be useful to rewrite the numerator of Γ_{fin}^μ making again use of relations (1.53a)-(1.53d), but in a space with $\omega = 2$. In this process also the Gordon identities (B.4a, B.4b) will

be useful:

$$\begin{aligned}
N_{fin}^\mu(p, q) &= \gamma^\rho [(1-u)\not{p} - v\not{q} + m_\mu] \gamma^\mu [(1-v)\not{q} - u\not{p} + m_\mu] \gamma_\rho \\
&= [(1-u)p_\alpha - vq_\alpha] [(1-v)q_\beta - up_\beta] \gamma^\rho \gamma^\alpha \gamma^\mu \gamma^\beta \gamma_\rho + m_\mu^2 \gamma^\rho \gamma^\mu \gamma_\rho \\
&\quad + m [(1-v)q_\alpha - up_\alpha] \gamma^\rho \gamma^\mu \gamma^\alpha \gamma_\rho + m [(1-u)p_\alpha - vq_\alpha] \gamma^\rho \gamma^\alpha \gamma^\mu \gamma_\rho \\
&= -2 [(1-u)\not{p} - v\not{q}] \gamma^\mu [(1-v)\not{q} - u\not{p}] - 2m_\mu^2 \gamma^\mu \\
&\quad + 4m(1-2v)q^\mu + 4m(1-2u)p^\mu \\
&\doteq -2(1-u)(1-v) \left[m_\mu^2 \gamma^\mu + \not{k}^2 \gamma^\mu + 4im\sigma^{\mu\alpha}(q-p)_\alpha \right] - 2(1+uv)m_\mu^2 \gamma^\mu \\
&\quad + 2m_\mu v(1-v)(4i\sigma^{\mu\alpha}q_\alpha + m_\mu \gamma^\mu) + 2m_\mu u(1-u)(-4i\sigma^{\mu\alpha}p_\alpha + m_\mu \gamma^\mu) \\
&\quad + 4m(1-2u)(m_\mu \gamma^\mu - 2i\sigma^{\mu\alpha}p_\alpha) + 4m(1-2v)(m_\mu \gamma^\mu + 2i\sigma^{\mu\alpha}q_\alpha) \\
&\doteq 2m_\mu^2 [2(1-u-v) - (u+v)^2] \gamma^\mu - 2\not{k}^2(1-u)(1-v)\gamma^\mu \\
&\quad + 8im_\mu \sigma^{\mu\alpha} \{ [u - v(u+v)] q_\alpha - [v - u(u+v)] p_\alpha \}
\end{aligned} \tag{1.58}$$

The basic result of the previous computation is to split $\Gamma_{fin}^\mu(p, q)$ into two contributions, one proportional to γ^μ and the other one proportional to $\sigma^{\mu\alpha}$, namely:

$$\Gamma_{fin}^\mu(p, q) \doteq \gamma^\mu F_1(k^2) + i\sigma^{\mu\alpha} \frac{k_\alpha}{m_\mu} F_2(k^2) \equiv \Gamma_1^\mu + \Gamma_2^\mu \tag{1.59}$$

where $F_1(k^2)$ and $F_2(k^2)$ are called *form factors*. In the limit of $k^2 \rightarrow 0$, we have $F_1(0) = 1$ and $F_2(0) = 0$, thus eq. (1.59) retraces the Dirac's result. Since the form factors contain the complete information about the interaction between the muon and the photon, they should, in particular, contain the muon electric and magnetic couplings. It is possible to prove that $F_1(k^2)$ appears in the relations that describe the behavior of muon in an external electric field. On the contrary, the description of the magnetic moment interaction $U(\mathbf{x})$, in the Born approximation, between a muon and an external magnetic field involves both form factors:

$$U(\mathbf{x}) = \boldsymbol{\mu} \cdot \mathbf{B}(\mathbf{x}) \tag{1.60}$$

where [7]

$$\boldsymbol{\mu} = -\frac{e}{m} [F_1(0) + F_2(0)] \mathbf{S} \tag{1.61}$$

comparing with the standard form

$$\boldsymbol{\mu} = -\frac{g_\mu \mu_B}{\hbar} \mathbf{S} \tag{1.62}$$

which is nothing but eq. (1.14) rearranged for the muon case. For the Landé g-factor we find:

$$g_\mu = 2 [F_1(0) + F_2(0)] = 2 + 2F_2(0) \tag{1.63}$$

Therefore, the form factor $F_2(k^2)$ is equal to the anomalous magnetic moment of the muon. For this reason, to evaluate the one-loop QED contribution to anomalous magnetic moment, we have to consider the only terms of eq (1.58) proportional to $\sigma^{\mu\alpha}$, which turns out to be both ultraviolet and infrared finite:

$$\Gamma_2^\mu(k^2) \doteq \frac{-8im_\mu\alpha}{4\pi} \int_0^1 du \int_0^{1-u} dv \frac{[u-v(u+v)]\sigma^{\mu\alpha}q_\alpha - [v-u(u+v)]\sigma^{\mu\alpha}p_\alpha}{u(1-u)p^2 + v(1-v)q^2 - (u+v)m_\mu^2 - 2uvp \cdot q} \quad (1.64)$$

computing this integral for on-shell particles:

$$\begin{aligned} \Gamma_2^\mu(0) &\doteq \frac{2im_\mu\alpha}{\pi} \int_0^1 du \int_0^{1-u} dv \frac{[u-v(u+v)]\sigma^{\mu\alpha}q_\alpha - [v-u(u+v)]\sigma^{\mu\alpha}p_\alpha}{(u+v)^2m_\mu^2} \\ &\doteq \frac{2i\alpha}{\pi m_\mu} \left(\sigma^{\mu\alpha}q_\alpha \int_0^1 du \int_0^{1-u} dv \frac{u-v(u+v)}{(u+v)^2} - \sigma^{\mu\alpha}p_\alpha \int_0^1 du \int_0^{1-u} dv \frac{v-u(u+v)}{(u+v)^2} \right) \\ &\doteq \frac{2i\alpha}{\pi m_\mu} \left(\frac{\sigma^{\mu\alpha}q_\alpha}{4} - \frac{\sigma^{\mu\alpha}p_\alpha}{4} \right) \\ &\doteq \frac{i\alpha}{2\pi m_\mu} \sigma^{\mu\alpha}k_\alpha \end{aligned} \quad (1.65)$$

Comparing the previous equation with eq. (1.59), we finally obtain the famous Schwinger's result:

$$F_2(0) = \frac{\alpha}{2\pi} \approx (1.1614097324 \pm 3) \times 10^{-3} \quad (1.66)$$

Hence the mass independent correction is $A_1^{(2)} = 1/2$ while the mass dependent corrections are $A_2^{(2)}(m_\mu/m_l) = A_3^{(2)}(m_\mu/m_e, m_\mu/m_\tau) = 0$, with m_l equal to m_e or m_τ . It follows that one-loop contribution is

$$C_1 = \frac{1}{2} \quad (1.67)$$

We will not report the calculations for all the other QED contributions, but only the results.

C₂: The two-loop contribution

We will discuss now on the two-loop QED correction to the muon anomalous magnetic moment. The coefficient C_2 is equal to:

$$C_2 = A_1^{(4)} + A_2^{(4)}(m_\mu/m_e) + A_2^{(4)}(m_\mu/m_\tau) + A_3^{(4)}(m_\mu/m_e, m_\mu/m_\tau) \quad (1.68)$$

At fourth order (e^4), there are seven diagrams contributing to $A_1^{(4)}$. In addition, at this order in the perturbative expansion the anomalous magnetic moment becomes dependent

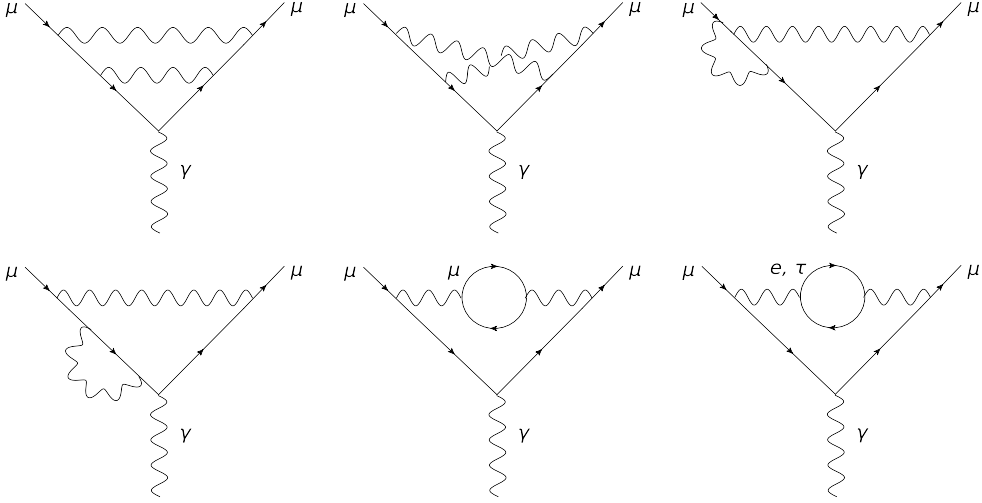


Figure 1.3: Two-loop QED correction diagrams. The mirror reflections of the third and fourth diagrams are not shown.

on the masses of all charged particles through the vacuum polarization diagrams. Just one diagram contributes to $A_2^{(4)}(m_\mu/m_e)$ and one to $A_2^{(4)}(m_\mu/m_\tau)$. There are not two-loop diagrams containing both virtual electrons and taus, thus $A_3^{(4)}(m_\mu/m_e, m_\mu/m_\tau) = 0$. The coefficient $A_1^{(4)}$ is:

$$[44] \quad A_1^{(4)} = \frac{197}{144} + \frac{\pi^2}{12} + \frac{3}{4}\zeta(3) - \frac{\pi^2}{2} \ln 2 = -0.328478965579... \quad (1.69)$$

where $\zeta(s)$ is the Riemann zeta function of arguments s .

It is convenient to sketch of the calculation of two-loop diagrams with the vacuum polarization subgraph, from which we obtain $A_2^{(4)}(m_\mu/m_l)$, with $l = e, \tau$, because this procedure will be useful afterwards. We have to apply Feynman rules to the last diagram of figure 1.3, but preliminary it is necessary to replace the leading-order propagator of the inner photon, with the following one [8]

$$\begin{aligned} D_{\mu\nu}(k) &= \frac{-ig_{\mu\nu}}{k^2} + \frac{(-i)g_{\mu\rho}}{k^2} [-i(k^2 g^{\mu\nu} - k^\mu k^\nu) \Pi(k^2)] \frac{(-i)g_{\sigma\nu}}{k^2} + \dots \\ &= \frac{-ig_{\mu\nu}}{k^2} + \frac{ig_{\mu\rho}}{k^4} (k^2 \delta^\mu_\nu - k^\rho k_\nu) \Pi(k^2) + \dots \\ &= \frac{-ig_{\mu\nu}}{k^2} (1 - \Pi(k^2)) - \frac{ik^\mu k_\nu}{k^4} + \dots \end{aligned} \quad (1.70)$$

which takes into account the photon self-energy tensor, consistent with the electromag-

netic gauge invariance. Thus, first-order correction to the photon propagator is

$$\begin{aligned} D_{\mu\nu}(k) &= \frac{-ig_{\mu\nu}}{k^2} (1 - \Pi(k^2)) \\ &\stackrel{o(\alpha)}{=} \frac{-ig_{\mu\nu}}{k^2} (1 - [\Pi(k^2) - \Pi(0)]) \end{aligned} \quad (1.71)$$

Making use of the Taylor expansion, the eq. (1.71) suggests that the electric charge can be replaced by an energy-momentum scale dependent *running charge*

$$e^2 \rightarrow e^2(k^2) = \frac{e^2}{1 + [\Pi(k^2) - \Pi(0)]} \quad (1.72)$$

which in terms of the fine-structure-constant $\alpha = e^2/4\pi$ reads

$$\alpha \rightarrow \alpha_{eff}(k^2) = \frac{\alpha_0}{1 + [\Pi(k^2) - \Pi(0)]} = \frac{\alpha_0}{1 - \Delta\alpha(k^2)} \quad (1.73)$$

where $\alpha_0 = \alpha$ is the fine-structure-constant in the Thomson limit.

Coming back to photon first-order correction (1.71), one can notice that the first addend accounts for a term corresponding to the one-loop correction, hence the two-loop correction is

$$\begin{aligned} \Gamma^\mu(p, q) &\doteq \frac{ie^2}{(2\pi)^4} \int d^4l \gamma^\rho (\not{l} + \not{p} + m_\mu) \gamma^\mu (\not{l} + \not{q} + m_\mu) \gamma_\rho \\ &\times \frac{\Pi(l^2) - \Pi(0)}{[(l+p)^2 - m_\mu^2 + i\varepsilon] [(l+q)^2 - m_\mu^2 + i\varepsilon] (l^2 + i\varepsilon)} \end{aligned} \quad (1.74)$$

Because of the analyticity (deriving from causality) the photon self-energy function satisfies the subtracted dispersion relation below:

$$\Pi(l^2) - \Pi(0) = \frac{l^2}{\pi} \int_{s_0}^{\infty} ds \frac{Im\Pi(s + i\varepsilon)}{s(s - l^2 + i\varepsilon)} \quad (1.75)$$

where s_0 refers to the lowest invariant squared mass of the fermion e and τ that can be produced in a decay of the virtual off-shell photons with invariant mass l^2 . This means that s_0 is equal to $4m_e^2$ or $4m_\tau^2$.

Due to the perturbative nature of the QED, we know that [9]

$$Im\Pi(s + i\varepsilon) = \frac{\alpha}{3} \sqrt{1 - \frac{4m_l^2}{s + i\varepsilon}} \left(1 + \frac{2m_l^2}{s + i\varepsilon} \right) \quad (1.76)$$

where m_l is the mass of the lepton circulating on the loop. Putting together eqq. (1.74), (1.75) and (1.76) and integrating them, it possible to show that the mass-dependent

coefficient $A_2^{(4)}(m_\mu/m_l)$, first exactly calculated in 1966 by H. Elend [10] [11], is

$$A_2^{(4)}(1/x) = -\frac{25}{36} - \frac{\ln x}{3} + x^2(4 + 3 \ln x) + x^4 \left[\frac{\pi^2}{3} - 2 \ln x \ln \left(\frac{1}{x} - x \right) - Li_2(x^2) \right] \\ + \frac{x}{2} (1 - 5x^2) \left[\frac{\pi^2}{2} - \ln x \ln \left(\frac{1-x}{1+x} \right) - Li_2(x) + Li_2(-x) \right] \quad (1.77)$$

where $x = m_l/m_\mu$ and $m_l = m_e$ or $m_l = m_\tau$ and $Li_2(z) = -\int_0^z dt \ln(1-t)/t$ is the so called dilogarithm function. The previous formula can be used both for the case of the electron loop, $0 < x < 1$, and for the tau loop, $x > 1$. For $x = 1$ (muon loop) eq. (1.77) gives a non-null contribution, already part of $A_1^{(4)}$. Evaluating the value of eq. (1.77) with $x = m_\mu/m_e = 206.7682843$ (52), $m_\mu = 105.6583692$ (94) MeV and $m_\tau = 1776.99$ (29) MeV [12], one gets:

$$[13] \quad A_2^{(4)}(m_\mu/m_e) = 1.0942583120 \quad (83) \quad (1.78)$$

$$[13] \quad A_2^{(4)}(m_\mu/m_\tau) = 0.000078079 \quad (15) \quad (1.79)$$

The magnitude of two-loop diagram with the τ lepton, as calculated in eq (1.79), provides a relative contribution to a_μ^{QED} of 10^{-11} .

Adding up the values of eqq. (1.69), (1.78) and (1.79), we obtain:

$$C_2 = A_1^{(4)} + A_2^{(4)}(m_\mu/m_e) + A_2^{(4)}(m_\mu/m_\tau) = 0.765857425 \quad (17) \quad (1.80)$$

The error on $\delta C_2 = 1.7 \times 10^{-8}$ leads an uncertainty on a_μ^{QED} equal to 0.94×10^{-13} .

C₃: the three-loop contribution

There are more than one hundred diagrams involved in the three-loop contribution to muon $g - 2$. Their analytic computation was finally performed only in the nineties. The mass independent coefficient $A_1^{(6)}$ arises from 72 diagrams. The calculation started around the 1970 [14] and was then completed only in 1996 by E. Remiddi and collaborators [15], [16]. The result for $A_1^{(6)}$ reads:

$$A_1^{(6)} = \frac{28259}{5184} + \frac{1710}{810}\pi^2 - \frac{298}{9}\pi^2 \ln 2 + \frac{139}{18}\zeta(3) + \frac{100}{3} \left[Li_4\left(\frac{1}{2}\right) + \frac{1}{24} \ln^4 2 - \frac{\pi^2 \ln^2 2}{24} \right] \\ - \frac{239}{2160}\pi^4 + \frac{83}{72}\pi^4 - \frac{215}{24}\zeta(5) \\ = 1.1812414566... \quad (1.81)$$

The calculation of the coefficients $A_2^{(6)}(m_\mu/m_l)$ was done by E. Remiddi and S. La-

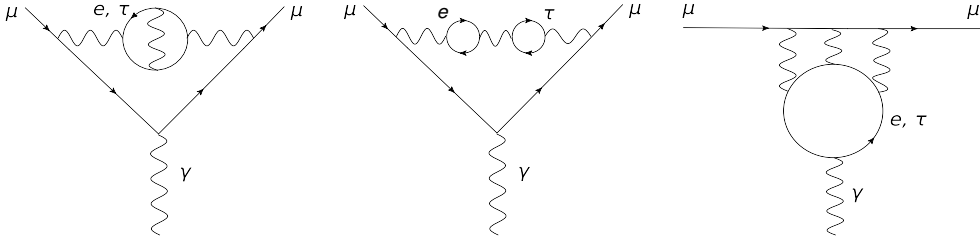


Figure 1.4: Examples of three-loop QED contribution to a_μ .

porta in 1993 [17]. These contributions can be split into two parts: the first, called $A_2^{(6)}(m_\mu/m_l, vp)$, containing e or τ vacuum polarization loops, arises from 36 diagrams; the other one called $A_2^{(6)}(m_\mu/m_l, lbl)$, receives contributions from 12 light-by-light (lbl) scattering diagrams with electron or tau loops. Traditionally, only lbl scattering diagrams with electron, muon and tau loops are included in the QED part of the muon magnetic anomaly. The light-by-light scattering diagrams mediated by the electron loops turn out to be particularly important: they represent the dominant part of light-by-light scattering contribution to a_μ . The results are:

$$[13] \quad A_2^{(6)}(m_\mu/m_e, vp, lbl) = 22.86838004 \quad (23) \quad (1.82)$$

$$[13] \quad A_2^{(6)}(m_\mu/m_\tau, vp, lbl) = 0.00036070 \quad (13) \quad (1.83)$$

At the sixth-order (α^6) also diagrams with both electron and tau loop are involved. The analytic calculation, available since 1999, but improved in recent years, yields:

$$[13] \quad A_3^{(6)}(m_\mu/m_e, m_\mu/m_\tau) = 0.00052776 \quad (11) \quad (1.84)$$

Combining the three-loop results all together, we obtain the complete three-loop QED coefficient:

$$\begin{aligned} C_3 &= A_1^{(6)} + A_2^{(6)}(m_\mu/m_e, vp, lbl) + A_2^{(6)}(m_\mu/m_\tau, vp, lbl) + A_3^{(6)}(m_\mu/m_e, m_\mu/m_\tau) \\ &= 24.05050996 \quad (29) \end{aligned} \quad (1.85)$$

The error $\delta C_3 = 29 \times 10^{-8}$, due to the experimental uncertainty of lepton masses, must be obtained taking into account the correlation of the addends. It represents an error contribution, to the uncertainty of a_μ^{QED} , equals to 0.38×10^{-14} . δC_3 is the lighter contribution to the uncertainty of the QED part of muon anomaly.

C₄: the four-loop contribution

The knowledge of four-loop correction is crucial in the comparison between the SM prediction and the experimental value of anomalous magnetic moment, because of its

magnitude is six-times larger than the present experimental uncertainty of a_μ . More than one thousand diagrams are involved in the evaluation of four-loop contribution. In contrast to the case of the lower orders calculation, the four-loop computations are fully numerical. The eight-order (e^8) correction has been obtained by T. Kinoshita and collaborators [18].

There are 891 four-loop diagrams contributing to $A_1^{(8)}$. According to S. Laporta, who had evaluated $A_1^{(8)}$ up to 1100 precision digits, we have [20]:

$$[13] \quad A_1^{(8)} = -1.9122457649... \quad (1.86)$$

The value of $A_2^{(8)}(m_\mu/m_e)$ depends on the calculation of other 469 diagrams and the result is:

$$[13] \quad A_2^{(8)}(m_\mu/m_e) = 132.6852 (60) \quad (1.87)$$

The term $A_2^{(8)}(m_\mu/m_\tau)$ represents a small contribution, of order of $\mathcal{O}(10^{-13})$ to a_μ^{QED} . T. Kinoshita quotes:

$$[13] \quad A_2^{(8)}(m_\mu/m_\tau) = 0.04234 (12) \quad (1.88)$$

Finally, there are 102 diagrams containing both e and τ loops. The value of value $A_3^{(8)}$ is:

$$[13] \quad A_3^{(8)}(m_\mu/m_e, m_\mu/m_\tau) = 0.06272 (4) \quad (1.89)$$

Adding up all these corrections in order to obtain the complete four-loop contribution to a_μ^{QED} , we get:

$$\begin{aligned} C_4 &= A_1^{(8)} + A_2^{(8)}(m_\mu/m_e) + A_2^{(8)}(m_\mu/m_\tau) + A_3^{(8)}(m_\mu/m_e, m_\mu/m_\tau) \\ &= 130.8780 (60) \end{aligned} \quad (1.90)$$

The error δC_4 adds up a small contribution, 1.8×10^{-13} to the theoretical uncertainty of a_μ^{QED} . However, it represents the heavier contribution to the uncertainty of the QED part of muon anomaly.

C₅: five-loop contribution

The complete calculation of tenth-order (e^{10}) QED contribution to the muon $g - 2$ is known thanks to a monumental work of T. Kinoshita and his collaborators: they have numerically evaluated all the sets of gauge-invariant diagrams that contribute to C_5 . The results of five-loop calculations are the following [13]:

$$\begin{aligned} A_1^{(8)} &= 9.168 (571) \\ A_2^{(8)}(m_\mu/m_e) &= 742.18 (87) \\ A_2^{(8)}(m_\mu/m_\tau) &= -0.068 (5) \\ A_3^{(8)}(m_\mu/m_e, m_\mu/m_\tau) &= 2.011 (10) \end{aligned}$$

Adding up all the terms, we obtain the complete five-loop correction to muon anomalous magnetic moment:

$$C_5 = 753.29 (1.04) \quad (1.92)$$

The uncertainty is attributed entirely to the statistical fluctuation in the Monte-Carlo integration of Feynman amplitudes. This result is 20 times more precise than the previous estimate, obtained with the previous leading-logarithmic approximation technique by Kinoshita himself [19]. The error δC_5 adds up a contribution of 0.7×10^{-13} to the uncertainty of a_μ^{QED} .

The complete QED contribution to a_μ

We are now able to estimate the quantum electrodynamics contribution to the muon anomalous magnetic moment. Using the latest Particle Data Group recommended value for the fine-structure-constant

$$\alpha^{-1} = 137.035999139 (31) \quad [0.23 \text{ ppb}] \quad (1.93)$$

we obtain the following value:

$$a_\mu^{QED} = 116584718869 (9)(19)(7)(31) \times 10^{-14} \quad (1.94)$$

where the uncertainties are due to the lepton mass ratios, the eighth-order term, the tenth-order term, and the value of α in (1.93), respectively. When combined in quadrature, these uncertainties yield $\delta a_\mu^{QED} = 37 \times 10^{-14}$. Therefore the finale QED result is

$$a_\mu^{QED} = (116584718869 \pm 37) \times 10^{-14} \quad (1.95)$$

1.2.2 The electroweak contribution to a_μ

The electroweak contribution (EW) to the anomalous magnetic moment of the muon is suppressed by the factor $(m_\mu/M_W)^2$ with respect to the QED effects [4]. It represents the smallest contribution to muon anomalous magnetic moment.

Is necessary to note that a_μ^{EW} also contains the hadronic corrections arising from the two-loop electroweak correction.

One-loop contribution

The one-loop EW contribution result to a_μ was published in 1972 by several authors [?]. Its analytic expression, obtained by computing Feynman diagrams as those in figure 1.5, reads

$$a_\mu^{EW}(\text{one loop}) = \frac{5G_\mu m_\mu^2}{24\sqrt{2}\pi^2} \left[1 + \frac{1}{5} (1 - 4\sin^2\theta_W)^2 + \mathcal{O}\left(\frac{m_\mu^2}{M_{Z,W,H}^2}\right) \right] \quad (1.96)$$

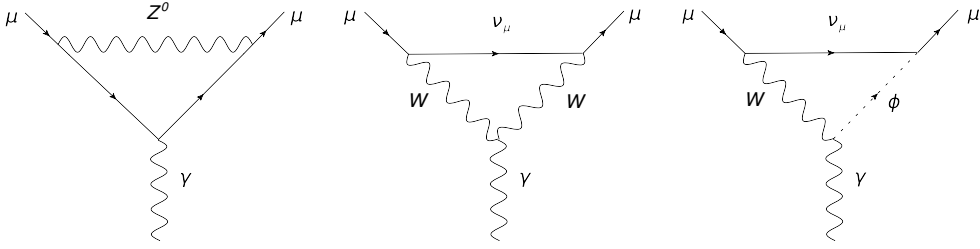


Figure 1.5: Examples of one-loop electroweak contribution to a_μ .

where $G_\mu = 1.16639(1) \times 10^{-5} \text{ GeV}^{-2}$, M_Z , M_W and M_H are the masses of the Z , W and Higgs bosons, and θ_W is the mixing angle. The magnitude of one-loop EW contribution to a_μ is

$$[21] \quad a_\mu^{EW}(\text{one loop}) = 194.8 \times 10^{-11} \quad (1.97)$$

The contribution of the Higgs diagram alone, given the Higgs mass $M_H = 125.09 \pm 0.21 \pm 0.11 \text{ GeV}$ [22], is smaller than 3×10^{-14} and can be safely neglected.

Two-loop contribution

Naively, one might expect that the two-loop electroweak contribution to be negligible, since of the relative strength $O(\alpha/\pi)$ with respect to the one-loop EW contribution. However, that is not the case. Kukhto [23] had shown that some two-loop electroweak contributions can be quite substantial because of the presence of terms enhanced by a factor of $\ln(M_{Z,W}/m_l)$, where m_l is a fermion mass scale much smaller than $M_{Z,W}$. Therefore the two-loop EW contribution must be included in the theoretical estimation of a_μ^{EW} , in order to obtain a value of the muon anomalous magnetic moment comparable with the experiments. The complete set of all the two-loop diagrams is quite large, it includes the total of 1678 diagrams. However, the diagrams with two or more scalar couplings to the muon line are suppressed by an extra factor of m_μ^2/M_W^2 and can be discarded.

The $a_\mu^{EW}(\text{two loop})$ can be divided into fermionic and bosonic part: the former includes all two-loop EW corrections containing only fermion loops, while all the other contributions have been included into the latter. Taking into account also the contribution of hadronic γ - Z mixing diagrams, which are suppressed by a factor $(1 - 4 \sin^2 \theta_W)$ both for quarks and leptons, the two-loop EW contribution is:

$$[24] \quad a_\mu^{EW}(\text{two loop}) = -41.2(2.0) \times 10^{-11} \quad (1.98)$$

the contribution of hadronic γ - Z mixing diagrams to the two-loop EW correction is 0.4×10^{-11} .

The hadronic leading contribution to a_μ therefore is a small fraction of the total SM prediction for the muon $g-2$ anomaly, but is very large when compared with the current experimental uncertainty $\delta a_\mu^{exp} = 63 \times 10^{-11}$ [26]. Indeed, δa_μ^{exp} is less than 1% of a_μ^{HLO} , justifying our interest for precisely estimating this contribution.

The evaluation of the diagram, figure 1.6, involves long-distance Quantum Chromodynamics (QCD) interactions, for which perturbative theory does not work. However, as it is well known, one can rely on the dispersion representation of the photon propagator and the optical theorem, which relate the hadronic vacuum polarization contribution to a_μ with the measured e^+e^- annihilation cross-section into hadrons. In principle, this technique allows to account for the effects of strong interactions exactly. Such an approach strongly relies on the experimental results, requiring many high-precision measurements of the $e^+e^- \rightarrow hadrons$ cross-sections. This dispersive approach was proposed by Bouchiat and Michel [27]. In the following we will retrace the calculation in order to obtain their formula.

For the inner photon propagator, we use the approximation obtained in eq. (1.71) by replacing the QED polarization function with the unknown QCD polarization function, which again satisfy the subtracted dispersion relation (1.75):

$$D_{\mu\nu}(k) = \frac{-ig_{\mu\nu}}{k^2} \rightarrow \frac{-ig_{\mu\nu}}{k^2} (1 - [\Pi_{had}(k^2) - \Pi_{had}(0)]) \quad (1.102)$$

Applying now the Feynman rules to figure 1.6, we get

$$\bar{u}(q)\Gamma_{had}^\mu(q,p)u(p) = \int \frac{d^4l}{(2\pi)^4} \bar{u}(q) (-ie\gamma^\sigma) S(l+k)\gamma^\mu S(l) (-ie\gamma^\rho) u(p) D_{\rho\sigma} \quad (1.103)$$

Taking into account only the correction to the photon-muon vertex due to the second addend of equation (1.102), we have:

$$\begin{aligned} \Gamma_{had}^\mu(p,q) &\doteq \frac{ie^2}{(2\pi)^4} \int d^4l \gamma^\rho (\not{l} + \not{p} + m_\mu) \gamma^\mu (\not{l} + \not{q} + m_\mu) \gamma_\rho \\ &\times \frac{\Pi_{had}(l^2) - \Pi_{had}(0)}{[(l+p)^2 - m_\mu^2 + i\varepsilon] [(l+q)^2 - m_\mu^2 + i\varepsilon] (l^2 + i\varepsilon)} \end{aligned} \quad (1.104)$$

which corresponds to the eq. (1.74) rearranged to represent the QCD case. Using the subtracted dispersion relation we obtain

$$\begin{aligned} \Gamma_{had}^\mu(p,q) &\doteq \frac{ie^2}{(2\pi)^4} \int d^4l \frac{\gamma^\rho (\not{l} + \not{p} + m_\mu) \gamma^\mu (\not{l} + \not{q} + m_\mu) \gamma_\rho}{[(l+p)^2 - m_\mu^2 + i\varepsilon] [(l+q)^2 - m_\mu^2 + i\varepsilon] (l^2 + i\varepsilon)} \\ &\times \frac{l^2}{\pi} \int_0^\infty ds \frac{Im\Pi_{had}(s+i\varepsilon)}{s(s-l^2+i\varepsilon)} \end{aligned} \quad (1.105)$$

exchanging the integration order is crucial in order to solve the integral

$$\begin{aligned} \Gamma_{had}^\mu(p, q) &\doteq \frac{ie^2}{(2\pi)^4} \int_0^\infty \frac{ds}{s\pi} \text{Im}\Pi_{had}(s+i\varepsilon) \\ &\times \int d^4l \frac{\gamma^\rho(\not{l} + \not{p} + m_\mu)\gamma^\mu(\not{l} + \not{q} + m_\mu)\gamma_\rho}{[(l+p)^2 - m_\mu^2 + i\varepsilon][(l+q)^2 - m_\mu^2 + i\varepsilon](s-l^2 + i\varepsilon)} \end{aligned} \quad (1.106)$$

The inner integral is similar to that one we have previously used to calculate the Schwinger result: the denominator is different, since of photon four-momentum is rescaled with the s variable, that can be somehow interpreted as a photon mass. We already know the prescription needed to solve this integral: apply the formula (A.1) in order to simplify the denominator, perform then a shift and as last step rewrite the numerator in the the form $\gamma^\mu \cdot A + i\sigma^{\mu\nu}k_\nu \cdot B$ where A and B are the coefficients. Again, we are interested in the value of the coefficient B , because of its direct connection to the muon anomalous magnetic moment. This recipe brings us to

$$\begin{aligned} \Gamma_{had}^\mu &\doteq \frac{\alpha}{\pi^2} \frac{i\sigma^{\mu\nu}}{m_\mu} k_\nu \int_0^\infty \frac{ds}{s} \text{Im}\Pi_{had}(s+i\varepsilon) \\ &\times \int dx dy dz \delta(x+y+z-1) \frac{m_\mu^2(1-z)z}{m_\mu^2(1-z)^2 - k^2xy + sz} \end{aligned} \quad (1.107)$$

Taking into account that the outer photon is real, i.e. $k^2 = 0$, we get

$$\begin{aligned} \Gamma_{had}^\mu &\doteq \frac{\alpha}{\pi^2} \frac{i\sigma^{\mu\nu}}{m_\mu} k_\nu \int_0^\infty \frac{ds}{s} \text{Im}\Pi_{had}(s+i\varepsilon) \int dx dy dz \delta(x+y+z-1) \frac{m_\mu^2(1-z)z}{m_\mu^2(1-z)^2 + sz} \\ &= \frac{\alpha}{\pi^2} \frac{i\sigma^{\mu\nu}}{m_\mu} k_\nu \int_0^\infty \frac{ds}{s} \text{Im}\Pi_{had}(s+i\varepsilon) \int_0^1 dz \frac{m_\mu^2(1-z)z}{m_\mu^2(1-z)^2 + sz} \int_0^{1-z} dy \\ &= \frac{\alpha}{\pi^2} \frac{i\sigma^{\mu\nu}}{m_\mu} k_\nu \int_0^\infty \frac{ds}{s} \text{Im}\Pi_{had}(s+i\varepsilon) \int_0^1 dz \frac{(1-z)^2z}{(1-z)^2 + \frac{sz}{m_\mu^2}} \end{aligned} \quad (1.108)$$

The value of the previous equation can be easily checked in the limit $s = 0$, since we expect it must be equal to the Schwinger result. Applying the change of variable $x \equiv 1 - z$, eq. (1.108) yields

$$\begin{aligned} \Gamma_2^\mu &\doteq \frac{\alpha}{\pi^2} \frac{i\sigma^{\mu\nu}}{m_\mu} k_\nu \int_0^\infty \frac{ds}{s} \text{Im}\Pi_{had}(s+i\varepsilon) \int_0^1 dx \frac{x^2(1-x)}{x^2 + (1-x)\frac{s}{m_\mu^2}} \\ &\equiv \frac{\alpha}{\pi^2} \frac{i\sigma^{\mu\nu}}{m_\mu} k_\nu \int_0^\infty \frac{ds}{s} \text{Im}\Pi_{had}(s+i\varepsilon) K(s) \end{aligned} \quad (1.109)$$

The kernel function $K(s)$ is

$$K(s) = \int_0^1 dx \frac{x^2(1-x)}{x^2 + (s/m_\mu^2)(1-x)} \quad (1.110)$$

Therefore we can write the Bouchiat and Michel formula:

$$a_\mu^{HLO} = \frac{\alpha}{\pi^2} \int_0^\infty \frac{ds}{s} K(s) \text{Im}\Pi_{had}(s + i\varepsilon) \quad (1.111)$$

Using the optical theorem for $e^+e^- \rightarrow hadrons$ scattering process [7]

$$\sigma_{e^+e^- \rightarrow had}(s) = \frac{4\pi\alpha}{s} \text{Im}\Pi_{had}(s) \quad (1.112)$$

we are able to relate the hadronic leading order contribution to muon $g - 2$ with the cross-section of the e^+e^- annihilation into hadrons

$$a_\mu^{HLO} = \frac{1}{4\pi^3} \int_{4m_\pi^2}^\infty ds K(s) \sigma_{e^+e^- \rightarrow had}(s) = \frac{\alpha^2}{3\pi^2} \int_{4m_\pi^2}^\infty \frac{ds}{s} K(s) R(s) \quad (1.113)$$

The integration domain runs from the lower energy-state available to the annihilation process, namely a final state with a couple of pion, to infinity. The function $R(s)$ is the ratio of $\sigma_{e^+e^- \rightarrow had}(s)$ and the high-energy limit of the Born cross-section for μ -pair production, therefore $R(s) = \sigma_{e^+e^- \rightarrow had}(s)/(4\pi\alpha^2/3s)$. The kernel function $K(s)$ decreases monotonically with increasing s , and for large s it behaves as $m_\mu^2/3s$ to a good approximation. For this reason the low-energy region of the dispersive integral is enhanced by $\sim s^{-2}$. About 91% of the total contribution to a_μ^{HLO} is due to center-of-mass energies \sqrt{s} below 1.8 GeV and 73% of a_μ^{HLO} is covered by the two-pion final state, which is dominated by the $\rho(770)$ resonance [4] [46]. The e^+e^- annihilation cross-sections at low-energy have been measured by many experiments at Novosibirsk (OLYA, TOF, ND, CMD, CMD-2, SND) and Orsay (M3N, DM1, DM2), while at higher energies the total cross-section ratio $R(s)$ has been measured inclusively by the experiments $\gamma\gamma 2$, MARK I, DELCO, DASP, PLUTO, LENA, MD-1, CELLO, JADE, MARK-J, CLEO, Mac and BES. Perturbative QCD can be used to evaluate higher loop momenta contributions, thus at some energy-scale is possible to switch from experimental data to theoretical calculation.

The main problem of this method is that it relies on the cross-sections data of positron-electron annihilation from many different experiments and furthermore one has to take into account the existence of hadronic resonances (see figure 1.7). A detailed study of eq. (1.113) has shown that a prominent role among all datasets is played by the precise measurement of the cross-section of $e^+e^- \rightarrow \pi^+\pi^-$ performed by the CMD-2 collaboration at Novosibirsk, at values of \sqrt{s} between 0.61 GeV and 0.96 GeV [30].

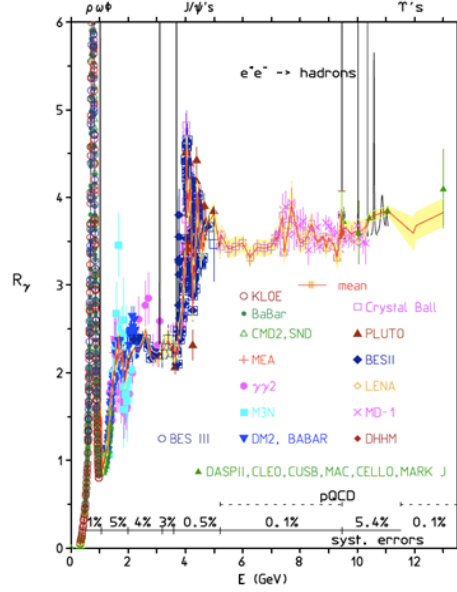


Figure 1.7: Cross-section of $e^+e^- \rightarrow \text{hadrons}$.

Particularly important are also the BABAR collaboration results for the other different final states produced from the e^+e^- annihilation ([31]-[36])

Using the experimental results, several authors have evaluated the dispersive integral of eq. (1.113). The most frequently quoted results in literature are

$$[48] \quad a_\mu^{HLO} = 6880.7 (41.4) \times 10^{-11} \quad (1.114a)$$

$$[57] \quad a_\mu^{HLO} = 6931 (34) \times 10^{-11} \quad (1.114b)$$

$$[50] \quad a_\mu^{HLO} = 6949 (42.7) \times 10^{-11} \quad (1.114c)$$

The results for the leading-order hadronic contribution are overlappable. The uncertainty of Jegerlehner's and Hagiwara's results is around 0.6%, eq. (1.114a) and eq. (1.114c) respectively. On the contrary, Davier's result, obtained from more restrictive and forced considerations, brings an error around 0.5%, eq. (1.114b)

Higher-order hadronic contribution to a_μ

Finally we will discuss the higher-order ($O(\alpha^3)$) hadronic contribution to a_μ , named a_μ^{HHO} , which can be written as:

$$a_\mu^{HHO} = a_\mu^{HHO}(vp) + a_\mu^{HHO}(lbl) \quad (1.115)$$

The first term grouped the contributions due to diagrams with vacuum polarization insertions, as shown in figures 1.8(a) and 1.8(b); the second term is the light-by-light

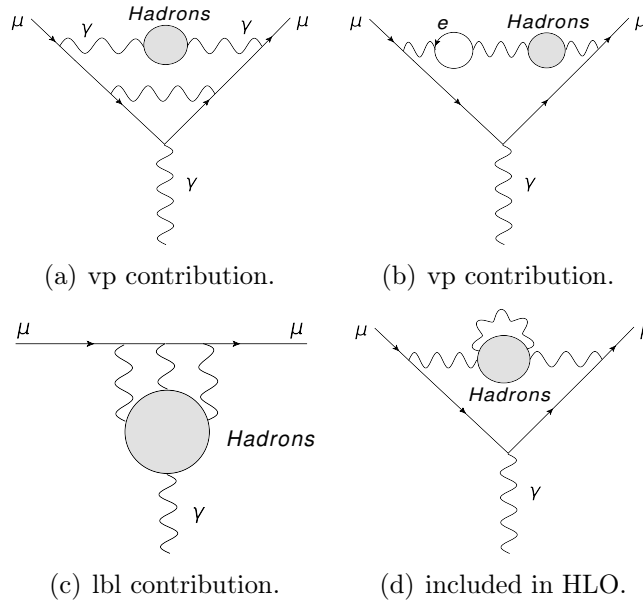


Figure 1.8: Examples of higher-order hadronic contribution to a_μ .

contribution, represented in figure 1.8(c). Note that the diagram shown in figure 1.8(d) has already been included in the leading-order hadronic contribution a_μ^{HLO} . The up to date values of these contribution are:

$$[28] \quad a_\mu^{HHO}(vp) = -98(1) \times 10^{-11} \quad (1.116a)$$

$$[48] \quad a_\mu^{HHO}(lbl) = 102(39) \times 10^{-11} \quad (1.116b)$$

Note that $a_\mu^{HHO}(vp)$ can be obtained using the same hadronic e^+e^- annihilation data, as described in the previous section. On the contrary seems that $a_\mu^{HHO}(lbl)$ cannot be expressed in term of experimental observables, hence its evaluation relies on purely theoretical consideration. This contribution has changed sign already three times in its troubled life and moreover different authors calculated even non-overlapping values [45]. The above $a_\mu^{HHO}(lbl)$ has been computed by Jegerlehner.

1.3 Theoretical and experimental value of a_μ

We have now all the ingredients to understand why the muon anomalous magnetic moment represents a possible indication of failure of the Standard Model. In this section we will collect all the theoretical results, presented formerly, to determine the SM prediction of a_μ . Afterwards we will briefly explain how a_μ is determined experimentally. Finally, we will make a comparison between the theoretical and the experimental results.

1.3.1 The theoretical value of a_μ

The theoretical value of muon anomalous magnetic moment is obtained summing up the following contributions

$$a_\mu^{SM} = a_\mu^{QED} + a_\mu^{EW} + a_\mu^{HLO} + a_\mu^{HHO}(vp) + a_\mu^{HHO}(lbl) \quad (1.117)$$

taking into account Jegerlehener results, of eqq. (1.114a) and (1.116b), we have

<i>contribution</i>	<i>value</i> (10^{-11})	<i>error</i> (10^{-11})
a_μ^{QED}	116584718.869	0.037
a_μ^{EW}	153.6	1
a_μ^{HLO}	6880.7	41.4
$a_\mu^{HHO}(vp)$	-98	1
$a_\mu^{HHO}(lbl)$	102	39

Summing up all SM contributions to a_μ as given in the previous table, we conclude that

$$a_\mu^{SM} = (11659175.7 \pm 5.7) \times 10^{-10} \quad [0.5 \text{ ppm}] \quad (1.118)$$

1.3.2 The experimental value of a_μ

It is now time to spend a few words about the experimental measurement used to obtain the empirical value of a_μ .

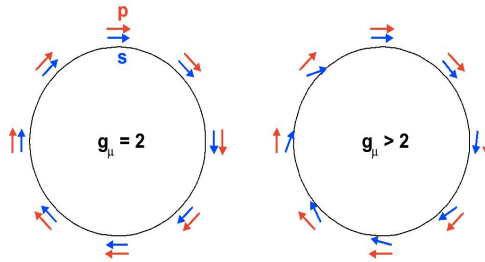


Figure 1.9: The spin precession relative to the momentum in the uniform magnetic field in case of $a_\mu = 0$ and $a_\mu > 0$.

The basic principle of the experiment is to observe the spin precessing of polarized muon relative to its momentum in an uniform magnetic field \mathbf{B} . In a space region in which there is an uniform magnetic field, muon will have a cyclotron motion, characterized by the cyclotron frequency ω_c :

$$\omega_c = -\frac{e\mathbf{B}}{m_\mu\gamma} \quad (1.119)$$

where γ is the usual Lorentz factor. At the same time, the muon spin precessing, with angular frequency $\boldsymbol{\omega}_s$, due to its anomalous magnetic moment, as shown in figure 1.9:

$$\boldsymbol{\omega}_s = -\frac{e\mathbf{B}}{m_\mu\gamma} - a_\mu\frac{e\mathbf{B}}{m_\mu} \quad (1.120)$$

The overall effect is a Larmor precession of the direction of the spin:

$$\boldsymbol{\omega}_a = \boldsymbol{\omega}_s - \boldsymbol{\omega}_c = -a_\mu\frac{e\mathbf{B}}{m_\mu} \quad (1.121)$$

In order to retain the muon in the ring an electrostatic focusing system is needed. Thus in addition to the magnetic field an electric quadrupole field in the plane normal to the particle orbit must be applied. In the presence of this electric field \mathbf{E} , the muon Larmor frequency is determined by the following equation, assuming the momentum is transverse to the magnetic field

$$\boldsymbol{\omega}_a = -\frac{e}{m_\mu} \left[a_\mu\mathbf{B} - \left(a_\mu - \frac{1}{\gamma^2 - 1} \right) \frac{\mathbf{B} \times \mathbf{E}}{c} \right] \quad (1.122)$$

Fortunately, the second term of equation (1.122), proportional to $\mathbf{B} \times \mathbf{E}$ vanishes if muon has the so-called "magic momentum" of 3.094 GeV ($\gamma = 29.3$). Hence, under this condition, the cyclotron frequency solely depends on the muon anomalous magnetic moment:

$$\boldsymbol{\omega}_a = -\frac{e}{m_\mu} a_\mu \mathbf{B} \quad (1.123)$$

The crucial result of previous equation is that the total precession frequency depends only on the anomalous magnetic moment a_μ .

The muon $g-2$ experiment are based on the production of muons from the decay of pions

$$\pi \rightarrow \mu + \nu_\mu \quad (1.124)$$

the polarization of muons is detected through the muon decay

$$\mu \rightarrow e + \nu_e + \nu_\mu \quad (1.125)$$

To produce a muon beam, a proton beam (accumulated in a proton storage ring) impinges upon a target material where pions are the most abundant secondary particles. Those pions are collected, momentum selected, and transported through a decay channel, along which they decay to muons. Muons are then injected into a storage ring with an extremely uniform magnetic field. The muon spin orientation can be observed by measuring the energy and arrival time of the high-energy positron/electron from muon decay with a calorimeter. Thanks to the parity violation of muon decay, the high-energy positron/electron in the muon rest frame are preferentially emitted parallel to the spin

orientation. In the laboratory frame, the positron/electron energy spectrum varies with the spin orientation with respect to the momentum. Therefore, the spin precession leads to the positron energy dependent event-rate modulation at the calorimeters. This event-rate modulation is shown in figure 1.10. By fitting this event-rate modulation, the experiments determine the frequency ω_a . To obtain the anomalous magnetic moment

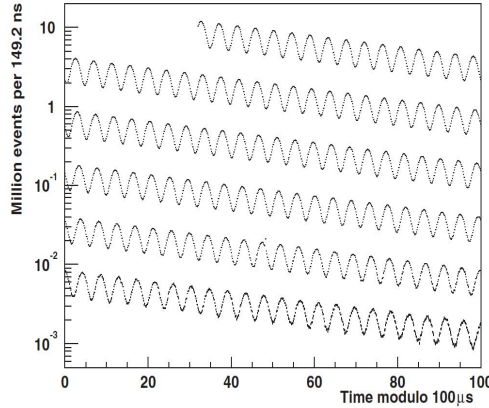


Figure 1.10: The modulation of the positron event-rate at the calorimeters.

from equation (1.123), the magnetic field needs to be known very precisely. The magnetic field in the muon storage region will be expressed in terms of the proton Larmor frequency $\omega_p = 2\mu_p B/\hbar$ where μ_p is the proton magnetic moment. Measuring the frequencies ω_a and ω_p it is possible to obtain the value of the muon anomaly, with the following relation

$$a_\mu = \frac{2\mu_p m_\mu}{e\hbar} \frac{\omega_a}{\omega_p} \quad (1.126)$$

Recalling equation (1.15), in the muon case:

$$\mu_\mu = -\frac{g_\mu}{2} \frac{e\hbar}{2m_\mu} = -(1 + a_\mu) \frac{e\hbar}{2m_\mu} \quad (1.127)$$

Combining eq. (1.126) with (1.127):

$$a_\mu = (1 + a_\mu) \frac{R}{\lambda} \quad (1.128)$$

where $R = \omega_a/\omega_p$ and $\lambda = \mu_\mu/\mu_p$. The quantity λ shows up since the magnetic field is measured thanks to the proton Larmor frequency. Precision experiments on the microwave spectrum of ground state muonium ($\mu^- e^+$) [37] performed at LAMPF at Los Alamos provide the needed result

$$\lambda = 3.18334539 (10) \quad (1.129)$$

Solving equation (1.128):

$$a_\mu = \frac{R}{\lambda - R} \quad (1.130)$$

The most accurate measure of a_μ^{exp} was obtained at E821, in Brookhaven. The experimental setup was made up by a toroid-shaped structure with a diameter of 14 meters, with the magnetic field of 1.45 T. The aperture of the pipe beam was 90 mm. Under this conditions, after each circle the muon spin axis changes by 12 arc seconds. At E821 the muon anomaly has been measured with 0.54 ppm precision. The result is [38]:

$$a_\mu^{exp} = (11659208.9 \pm 5.4 \pm 3.3) \times 10^{-10} \quad (1.131)$$

1.3.3 Standard Model Vs experiment

Now we are ready to understand why the anomalous magnetic moment of the muon represents one of the most interesting possible failure of our great theoretical apparatus, called Standard Model.

Comparing the Standard Model prediction and experimental value of muon anomalous magnetic moment, obtained in eqq. (1.118) and (1.131), in unit of 10^{-10} , we get:

$$\begin{array}{c} \hline \hline a_\mu^{exp} = 11659208.9 \pm 6.3 \\ a_\mu^{SM} = 11659175.7 \pm 5.7 \\ \hline \hline \Delta a_\mu = 33.2 \pm 6.3 \pm 5.7 \\ \hline \hline \end{array}$$

we get a non-null difference Δa_μ with a significant of 3.9σ .

Recalling that the theoretical value of muon $g - 2$ is not unique, due to the different results of the hadronic leading-order and higher-order contributions to muon anomaly, the difference between the theoretical and the experimental value swings from the lower limit of 3σ to the upper limit of 4σ . As said, our result has been obtained relying on the last outcomes of calculation by F. Jegerlehner.

Chapter 2

The novel approach to the leading hadronic contribution to muon $g-2$

The uncertainty associated to the theoretical value of the muon anomalous magnetic moment is due to all the uncertainties of the contributions to a_μ . However, as observed, some of them are negligible. The hadronic uncertainty instead is the main source of the SM uncertainty being comparable to the experimental one. This is the reason why the hadronic corrections have been kept under close scrutiny for several years.

An intense research program is ongoing aiming to improve the evaluation of the hadronic leading-order (HLO) contribution to a_μ . In this context, a group of Italian physicists has proposed a new method to determine with high precision the value of a_μ^{HLO} . The idea is to measure the running of the effective electromagnetic coupling in the space-like region by measuring the elastic scattering $\mu + e^- \rightarrow \mu + e^-$ that is a pure t-channel space-like process [39] [40].

The proposed method is based on eq. (1.111) evaluated exchanging the order of the integration:

$$\begin{aligned} a_\mu^{HLO} &= \frac{\alpha}{\pi^2} \int_0^1 dx x^2(1-x) \int_0^\infty \frac{ds}{s} \frac{Im\Pi_{had}(s+i\varepsilon)}{x^2 + (1-x)s/m_\mu^2} \\ &= \frac{\alpha}{\pi^2} \int_0^1 dx m_\mu^2 x^2 \int_0^\infty \frac{ds}{s} \frac{Im\Pi_{had}(s+i\varepsilon)}{\frac{x^2 m_\mu^2}{1-x} + s} \end{aligned} \quad (2.1)$$

By defining t as:

$$t(x) \equiv \frac{x^2 m_\mu^2}{x-1} < 0 \quad (2.2)$$

the dimension of the t variable is that of a squared momentum. It varies in the interval $t \in]-\infty, 0]$. Using the subtracted dispersion relation for the photon self-energy below:

$$\bar{\Pi}_{had}[t(x)] \equiv \Pi_{had}(t+i\varepsilon) - \Pi_{had}(0+i\varepsilon) = \frac{t}{\pi} \int_0^\infty ds \frac{Im\Pi_{had}(s+i\varepsilon)}{s(s-t+i\varepsilon)} \quad (2.3)$$

we obtain

$$a_\mu^{HLO} = \frac{\alpha}{\pi} \int_0^1 dx (x-1) \bar{\Pi}_{had}[t(x)] \quad (2.4)$$

The t variable is the argument of the photon self-energy function, hence can be identified to be exactly the Mandelstam's variable.

By inverting eq. (2.2) we get $x = (1 - \beta)(t/2m_\mu^2)$ with $\beta = (1 - 4m_\mu^2/t)^{1/2}$, we can write equation (2.4) in the t variable as

$$\begin{aligned} a_\mu^{HLO} &= \frac{\alpha}{\pi} \int_{-\infty}^0 dt \frac{1}{2m_\mu^2} \left[\frac{2m_\mu^2}{\beta t} - (1 - \beta) \right] \left[\frac{(1 - \beta)t}{2m_\mu^2} - 1 \right] \bar{\Pi}_{had}(t) \\ &= \frac{\alpha}{\pi} \int_{-\infty}^0 \frac{dt}{\beta t} \left(\frac{1 - \beta}{1 + \beta} \right)^2 \bar{\Pi}_{had}(t) \end{aligned} \quad (2.5)$$

It is a known expression, already being used in lattice QCD calculations of a_μ^{HLO} [58] [59]

The HLO contribution to a_μ in terms of the real and the imaginary part of $\bar{\Pi}_{had}[t(x)]$, which appears in eq. (2.4), can be written as [8]

$$\begin{aligned} a_\mu^{HLO} &= \frac{\alpha}{\pi} \int_0^1 dx (x-1) [Re\bar{\Pi}_{had}[t(x)] + iIm\bar{\Pi}_{had}[t(x)]] \\ &= \frac{\alpha}{\pi} \int_{t<0}^1 dx (x-1) Re\bar{\Pi}_{had}[t(x)] \end{aligned} \quad (2.6)$$

Recalling eq. (1.73) for the hadronic case and using the definition (2.3), we get:

$$\Delta\alpha_{had}[t(x)] = -Re\bar{\Pi}_{had}[t(x)] \quad (2.7)$$

The hadronic leading-order contribution to muon anomalous magnetic moment reads

$$a_\mu^{HLO} = \frac{\alpha}{\pi} \int_0^1 dx (1-x) \Delta\alpha_{had}[t(x)] \quad (2.8)$$

The analytic expression of $\Delta\alpha_{had}[t(x)]$ is unknown, cause of the non-perturbative character of the QCD at low-energy. However, it is possible to determine its expression by measuring the running of α :

$$\alpha(t) = \frac{\alpha(0)}{1 - \Delta\alpha(t)} \quad (2.9)$$

where $\alpha(0)$ is the fine-structure-constant in the Thomson limit. Moreover the expression of the shift of α , can be written as:

$$\Delta\alpha(t) = \Delta\alpha_{lep}(t) + \Delta\alpha_{had}(t) + \Delta\alpha_{top}(t) \quad (2.10)$$

$\Delta\alpha_{lep}(t)$, $\Delta\alpha_{had}(t)$ and $\Delta\alpha_{top}(t)$ respectively are the contributions due to leptons loops, light quarks loops and to the top quark loops. We separate the top quark contribution

from the others because at *top* energy-scale QCD can be calculated with perturbative techniques. Actually, at the energy scale of interest the *top* quark contribution to the running of α turns to be negligible.

Similarly the γ - Z weak contribution to the running of alpha, which should be included in eq. (2.10), turns out to be negligible too.

Hence, the hadronic shift $\Delta\alpha_{had}(t)$ can be calculated subtracting the purely leptonic part $\Delta\alpha_{lep}(t)$ to $\Delta\alpha(t)$. $\Delta\alpha_{lep}(t)$ can be calculated with the perturbative expansion order-by-order (known up to three-loop in QED [60]).

The hadronic and the leptonic contributions to the fine-structure-constant, as a functions of x are shown on left side of figure 2.1. To calculate their values we used the F. Jegerlehner's routine `hadr5n12` [30] [49], which uses $e^+e^- \rightarrow hadrons$ time-like data and perturbative QCD.

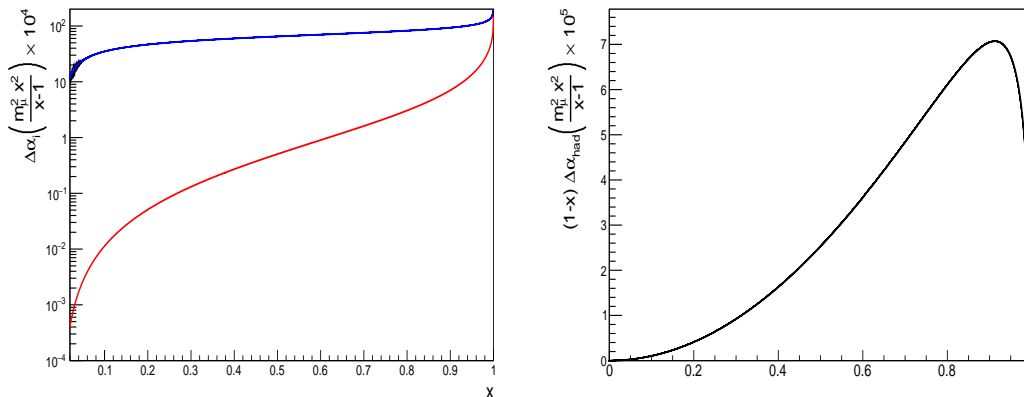


Figure 2.1: On the left, the plot shows $\Delta\alpha_{lep}[t(x)] \times 10^4$ (blue) and $\Delta\alpha_{had}[t(x)] \times 10^4$ (red). The plot on the right represents the integrand function of eq. (2.8).

2.1 μ - e scattering process

We have shown how by measuring the running of the fine-structure-constant $\Delta\alpha_{had}$ as a function of the transferred momentum would allow to determine a_μ^{HLO} . We have also seen how it would be possible to get $\Delta\alpha_{had}$ from measuring $\Delta\alpha(t)$ by subtracting the $\Delta\alpha_{lep}$ contribution.

In order to precisely measure $\Delta\alpha(t)$ one has to perform a dedicated experiment.

The μ - e elastic scattering differential cross-section would allow to precisely determine $\Delta\alpha(t)$ as a function of t since the scattering process involves only space-like transferred momenta (t -channel, $t < 0$). The μ - e elastic scattering is therefore much simpler than

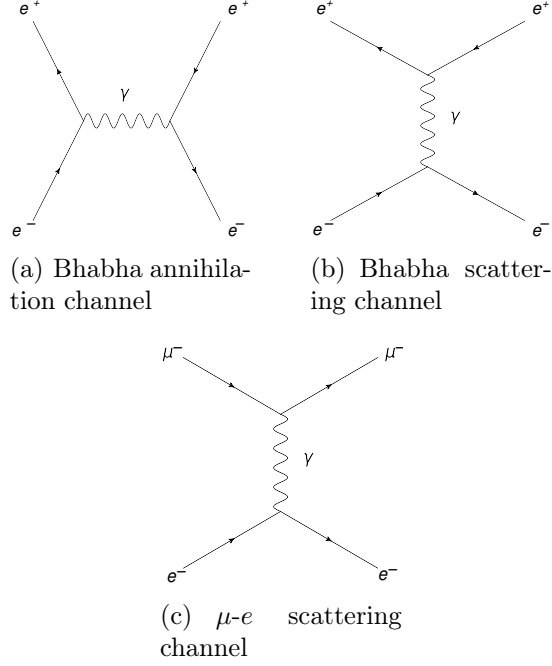


Figure 2.2: Bhabha and μ - e scattering processes.

the Bhabha, if considered as possible alternative. In fact, the Bhabha is both an annihilation and a scattering process, while the former is a pure scattering one.

The Feynman diagrams of the two processes are represented in figure 2.2.

In the following part we aim to evaluate the μ - e scattering cross-section in the Born approximation. By applying the Feynman rules to the diagram of 2.2(c), assuming the incoming states: electron with four-momentum p and spinor index r , and muon with four-momentum q and spinor index s ; and the outgoing states: an outgoing electron with four-momentum p' and spinor index r' , and an outgoing muon with four-momentum q' and spinor index s' , for the matrix element we can write:

$$\mathcal{M}_{r,r',s,s'}(p,p',q,q') = \bar{u}_{r'}(p') (-ie\gamma^\mu) u_r(p) D_{\mu\nu} \bar{u}_{s'}(q') (-ie\gamma^\nu) u_s(q) \quad (2.11)$$

Summing up over the spin indices the square modulus of the matrix element, we get:

$$\begin{aligned} |\mathcal{M}(p,p',q,q')|^2 &= \frac{1}{4} \sum_{r,r'} \sum_{s,s'} |\mathcal{M}_{r,r',s,s'}(p,p',q,q')|^2 \\ &= \frac{1}{4} \sum_{r,r'} \sum_{s,s'} \frac{e^4}{(p'-p)^4} g_{\mu\nu} g_{\rho\sigma} (\bar{u}_{r'}(p') \gamma^\mu u_r(p) \bar{u}_{s'}(q') \gamma^\nu u_s(q)) \\ &\quad \times (\bar{u}_r(p) \gamma^\rho u_{r'}(p') \bar{u}_s(q) \gamma^\sigma u_{s'}(q')) \end{aligned} \quad (2.12)$$

Using the completeness relation

$$\sum_{r=1,2} u_r(p) \otimes \bar{u}_r(p) = (\not{p} + m) \quad (2.13)$$

we obtain

$$|\mathcal{M}(p, p', q, q')|^2 = \frac{e^4}{4t^2} g_{\mu\nu} g_{\rho\sigma} \text{tr} [(\not{p}' + m_e) \gamma^\mu (\not{p} + m_e) \gamma^\rho] \text{tr} [(\not{q}' + m_\mu) \gamma^\nu (\not{q} + m_\mu) \gamma^\sigma] \quad (2.14)$$

where t represents the transferred momentum.

Considering terms with an even number of the γ^μ matrices (the trace of an odd number of γ matrices is equal to zero) and making use of eqq. (C.1) and (C.3) we get:

$$\begin{aligned} |\mathcal{M}(p, p', q, q')|^2 &= \frac{4e^4}{t^2} g_{\mu\nu} g_{\rho\sigma} (p'^\mu p^\rho + p'^\rho p^\mu + g^{\mu\rho} (m_e^2 - p' \cdot p)) \\ &\quad \times (q'^\nu q^\sigma + q'^\sigma q^\nu + g^{\nu\sigma} (m_\mu^2 - q' \cdot q)) \\ &= \frac{4e^4}{t^2} (p'_\nu p_\sigma + p'_\sigma + g_{\nu\sigma} (m_e^2 - p' \cdot p)) (q'^\nu q^\sigma + q'^\sigma q^\nu + g^{\nu\sigma} (m_\mu^2 - q' \cdot q)) \\ &= \frac{8e^4}{t^2} [(p' \cdot q') (p \cdot q) + (p' \cdot q) (p \cdot q') - m_\mu^2 (p' \cdot p) - m_e^2 (q' \cdot q) + 2m_e^2 m_\mu^2] \end{aligned} \quad (2.15)$$

It is useful to rewrite eq. (2.15) as a function of the Mandelstam's variables:

$$\begin{aligned} s &= (p + q)^2 = m_e^2 + m_\mu^2 + 2p \cdot q \\ t &= (p - p')^2 = 2m_e^2 - p \cdot p' \\ u &= (p - q')^2 = m_e^2 + m_\mu^2 - 2p \cdot q' \end{aligned} \quad (2.16)$$

and thereby

$$\begin{aligned} (p \cdot q) &= [p^2 + q^2 - (p + q)^2] / 2 = (s - m_e^2 - m_\mu^2) / 2 = (p' \cdot q') \\ (p \cdot q') &= (m_e^2 + m_\mu^2 - u) / 2 = (p' \cdot q) \\ (p \cdot p') &= (2m_e^2 - t) / 2 \\ (q \cdot q') &= (2m_\mu^2 - t) / 2 \end{aligned} \quad (2.17)$$

In such a manner the amplitude in eq. (2.15) becomes

$$\begin{aligned} |\mathcal{M}(p, p', q, q')|^2 &= \frac{8e^4}{t^2} \left[\frac{(s - m_e^2 - m_\mu^2)^2}{4} + \frac{(m_e^2 + m_\mu^2 - u)^2}{4} \right. \\ &\quad \left. - m_\mu^2 \left(\frac{2m_e^2 - t}{2} \right) - m_e^2 \left(\frac{2m_\mu^2 - t}{2} \right) + 2m_e^2 m_\mu^2 \right] \end{aligned} \quad (2.18)$$

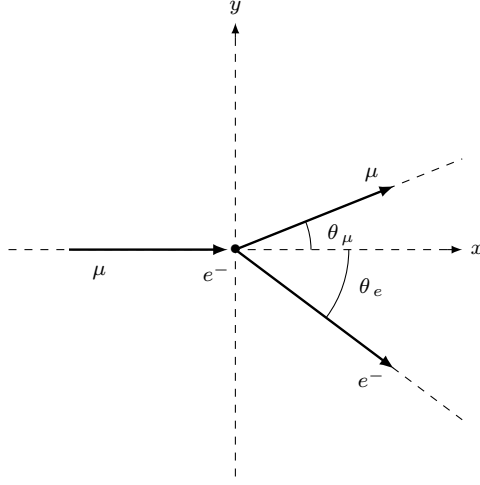


Figure 2.3: μ - e scattering in the laboratory rest frame.

Using the relation between the Mandelstam's variables:

$$s + t + u = 2(m_e^2 + m_\mu^2) \quad (2.19)$$

we obtain the amplitude $|\mathcal{M}(p, p', q, q')|^2$ as a function of them:

$$\begin{aligned} |\mathcal{M}(s, t)|^2 &= \frac{8e^4}{t^2} \left[\frac{(s - m_e^2 - m_\mu^2)^2}{4} + \frac{(s + t - m_e^2 - m_\mu^2)^2}{4} + \frac{tm_\mu^2}{2} + \frac{tm_e^2}{2} \right] \\ &= \frac{2e^4}{t^2} (t^2 + 2st + 2s^2 - 4sm_e^2 - 4sm_\mu^2 + 2m_e^4 + 2m_\mu^4 + 4m_e^2m_\mu^2) \end{aligned} \quad (2.20)$$

To evaluate the differential cross-section, we have to use the Quantum Field Theory golden rule [9]:

$$\begin{aligned} d\sigma &= \frac{1}{4} [(p \cdot q)^2 - m_e^2 m_\mu^2]^{-1/2} |\mathcal{M}(p, p', q, q')|^2 \\ &\quad \times (2\pi)^4 \delta(p' + q' - p - q) \frac{d\mathbf{p}'}{[(2\pi)^3 2E'_e]} \frac{d\mathbf{q}'}{[(2\pi)^3 2E'_\mu]} \end{aligned} \quad (2.21)$$

which is Lorentz invariant.

We have to choose a particular reference frame to solve eq. (2.21). Assuming the

muon hits the electron at rest in the laboratory frame one can write:

$$\begin{aligned}
\text{incoming electron:} & \quad \mathbf{p} = 0 & E_e &= m_e \\
\text{incoming muon:} & \quad \mathbf{q} \neq 0 & E_\mu &= \sqrt{\mathbf{q}^2 + m_\mu^2} \\
\text{outgoing electron:} & \quad \mathbf{p}' \neq 0 & E'_e &= \sqrt{\mathbf{p}'^2 + m_e^2} \\
\text{outgoing muon:} & \quad \mathbf{q}' = \mathbf{q} - \mathbf{p}' & E'_\mu &= E_\mu + m_e - E'_e
\end{aligned}$$

In this reference frame the Mandelstam's variables read

$$\begin{aligned}
s &= (p + q)^2 = m_e^2 + m_\mu^2 + 2E_\mu m_e \\
t &= (p - p')^2 = -2m_e (E'_e - m_e) \\
u &= (p - q')^2 = m_e^2 - m_e (m_e + 2E_\mu - 2E'_e)
\end{aligned} \tag{2.22}$$

We can now integrate the golden rule in the laboratory rest frame:

$$d\sigma = \frac{|\mathcal{M}(s, t)|^2}{16\pi^2 flux(s)} \int d\mathbf{p}' d\mathbf{q}' \frac{\delta(\mathbf{p}' + \mathbf{q}' - \mathbf{q}) \delta(E'_\mu + E'_e - E_\mu - m_e)}{E'_\mu E'_e} \tag{2.23}$$

here $flux(s)$ stands for the energetic term, which appears in eq. (2.21), written as a function of the Mandelstam's variable s :

$$flux = 4 \left[\left(\frac{s - m_e^2 - m_\mu^2}{2} \right)^2 - m_e^2 m_\mu^2 \right]^{1/2} \tag{2.24}$$

Using the Dirac delta function, we are able to integrate eq. (2.23) in the variable \mathbf{q}'

$$\begin{aligned}
d\sigma &= \frac{|\mathcal{M}(s, t)|^2}{16\pi^2 flux(s)} \int d\mathbf{p}' \frac{\delta(E'_\mu + E'_e - E_\mu - m_e)}{E'_\mu E'_e} \\
&= \frac{|\mathcal{M}(s, t)|^2}{16\pi^2 flux(s)} \int d|\mathbf{p}'| d\Omega(\theta_e, \phi) \frac{|\mathbf{p}'|^2 \delta(E'_\mu + E'_e - E_\mu - m_e)}{E'_\mu E'_e}
\end{aligned} \tag{2.25}$$

In order to obtain the μ - e differential cross-section as a function of t , we have to integrate in the solid angle ($d\Omega$), makes use the Dirac delta function, and perform a change of variables to switch from the modulus of the scattered electron momentum to the Mandelstam's variable t . Since vector momentum conservation, we have:

$$\mathbf{q}' = \mathbf{q} - \mathbf{p}' \tag{2.26}$$

which square modulus is:

$$|\mathbf{q}'|^2 = |\mathbf{q}|^2 + |\mathbf{p}'|^2 - 2|\mathbf{q}||\mathbf{p}'| \cos \theta_e \tag{2.27}$$

making use of mass shell-relation

$$E'_\mu = \sqrt{E'^\mu_\mu + E'^\mu_e - m_e^2 - 2|\mathbf{q}||\mathbf{p}'| \cos \theta_e} \quad (2.28)$$

Thus we can computing the angular Dirac delta function:

$$\begin{aligned} \delta(E'_\mu + E'_e - E_\mu - m_e) d\Omega(\theta_e, \phi) &= \frac{2\pi \delta(\cos \theta_e - \cos \theta) d(\cos \theta_e)}{\left| \frac{\partial(E_\mu + m_e - E'_e - E'_\mu(E'_e, \theta_e))}{\partial \cos \theta_e} \right|_{\cos \theta}} \\ &= \frac{2\pi \delta(\cos \theta_e - \cos \theta'_e) d(\cos \theta_e)}{\frac{|\mathbf{p}'||\mathbf{p}'|}{E_\mu + m_e - E'_e}} \end{aligned} \quad (2.29)$$

While, from the differential modulus of the scattered electron, we get:

$$d|\mathbf{p}'| = dE'_e \frac{E'_e}{\sqrt{E'^2_e - m_e^2}} = dE'_e \frac{E'_e}{|\mathbf{p}'|} = dt \frac{E'_e}{2m_e |\mathbf{p}'|} \quad (2.30)$$

Finally, we obtain the differential cross section in the laboratory rest frame:

$$\begin{aligned} d\sigma &= \frac{2|\mathcal{M}(s, t)|^2}{16\pi flux(s)} \int dt d(\cos \theta_e) \delta(\cos \theta_e - \cos \theta) \frac{E_\mu + m_e - E'_e}{2m_e |\mathbf{q}| E'_\mu} \\ &= \frac{2|\mathcal{M}(s, t)|^2}{16\pi flux(s)} \frac{dt}{2m_e |\mathbf{q}|} \end{aligned} \quad (2.31)$$

By algebraic manipulations is possible to write the previous equation as a function of the Mandelstam's variables as:

$$\frac{d\sigma}{dt} = \frac{2|\mathcal{M}(s, t)|^2}{16\pi flux(s)} \frac{1}{\sqrt{\lambda(s, m_e^2, m_\mu^2)}} \quad (2.32)$$

where $\lambda(s, m_e^2, m_\mu^2)$ is the *Källén function*:

$$\lambda(s, m_e^2, m_\mu^2) = [s^2 + m_e^4 + m_\mu^4 - 2s(m_e^2 + m_\mu^2) - 2m_e^2 m_\mu^2] \quad (2.33)$$

The explicit form of the μ - e scattering differential cross-section is:

$$\frac{d\sigma}{dt} = \frac{\pi\alpha^2}{t^2} \frac{(t^2 + 2st + 2s^2 - 4sm_e^2 - 4sm_\mu^2 + 2m_e^4 + 2m_\mu^4 + 4m_e^2 m_\mu^2)}{\sqrt{\left(\left(\frac{s-m_e^2-m_\mu^2}{2}\right)^2 - m_e^2 m_\mu^2\right) (s^2 + m_e^4 + m_\mu^4 - 2s(m_e^2 + m_\mu^2) + 2m_e^2 m_\mu^2)}} \quad (2.34)$$

where the dependence from the fine-structure-constant is explicit.

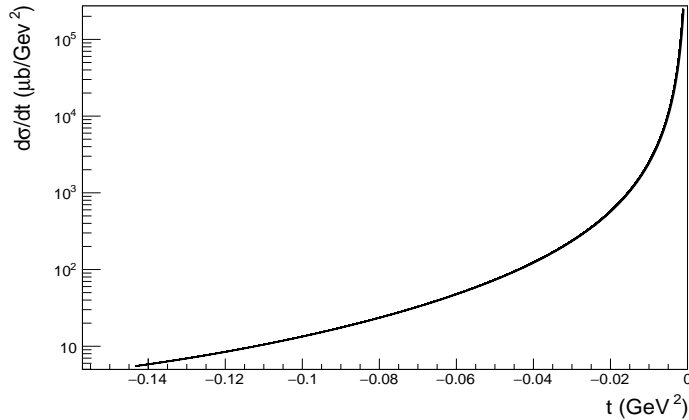


Figure 2.4: The Born approximation of the μ - e elastic cross section.

The differential cross-section is usually written as:

$$\frac{d\sigma}{dt} = \frac{\mathbf{C}}{flux(s)} \frac{|\mathcal{M}(s, t)|^2}{\sqrt{\lambda(s, m_e^2, m_\mu^2)}} \quad (2.35)$$

where \mathbf{C} is the conversion factor if natural units are used and masses and momenta are in GeV:

$$\mathbf{C} = 0.389379660 \text{ mbarn} \times \text{GeV}^2 \quad (2.36)$$

The μ - e differential cross-section in the Born approximation, computed in eq. (2.35), is represented in figure 2.4. The function goes to zero in the limit $t \rightarrow -\infty$, while its values grows for vanishing transferred momenta.

One may notice that eq. (2.35) is expressed in terms of the two Mandelstam's variables s and t . Therefore the differential cross-section as a function of the transferred momentum can be calculated for constant \sqrt{s} center of mass energy. Assuming an incoming muon energy of about 150 GeV, an ideal value to perform the μ - e experiments, it is possible to span the t region within $-0.142893 \leq t < 0 \text{ GeV}^2$. Integrating the differential cross-section in this t range, we obtain a total value of $\sigma = 245 \mu\text{b}$. One can observe that greater values of the incoming muon energy would just slightly increase the knowledge of the integrand function of eq. (2.8). The residual part of the integral, amounting to a remaining fraction of 13% of the total interval, can be calculated with pQCD and time-like data.

To precisely determine the running of the fine-structure-constant we have to calculate the differential cross-section taking into account the radiative corrections to the photon propagator. The first-order correction can be estimated by replacing the photon propagator with the photon self-energy function. We have already calculated it in eq.

(1.71) and (1.73). Making use of eq. (1.71), considering the first-order correction, the cross-section reads [40]:

$$\frac{d\sigma}{dt} = \left| \frac{\alpha(t)}{\alpha(0)} \right|^2 \frac{d\sigma_0}{dt} \quad (2.37)$$

where $d\sigma_0$ is the cross-section in the Born approximation that we have previously computed. Inverting this equation we gain:

$$\frac{d\sigma/dt}{d\sigma_0/dt} = \left| \frac{\alpha(t)}{\alpha(0)} \right|^2 \quad (2.38)$$

Therefore, measuring the μ - e differential elastic cross-section we can determine the running of α . Subtracting the leptonic running $\Delta\alpha_{lep}$ we can finally determine the purely hadronic running $\Delta\alpha_{had}$.

The figure 2.5 shows the effect of the hadronic and leptonic running on the cross-section with respect to the cross-section calculated considering just the leptonic contribution. Likely the precision of the first-order correction would not be precise enough to

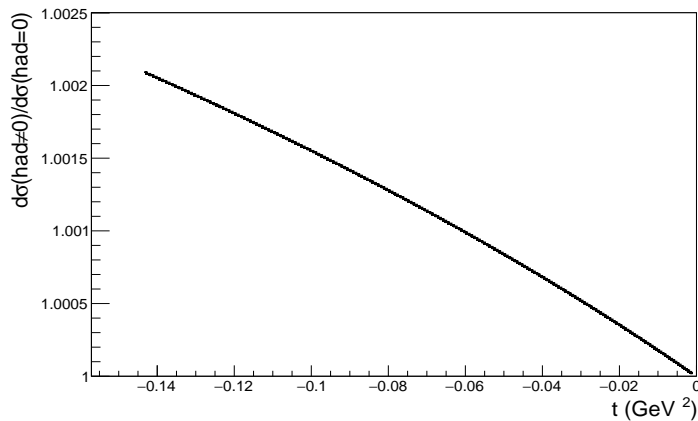


Figure 2.5: Ratio of the cross-section calculated with the hadronic and the leptonic running and the cross-section considering only leptonic one.

obtain the value of the hadronic running of alpha at the required precision level. It will be required to calculate the second-order correction of the μ - e differential cross-section.

2.2 Measuring the μ - e elastic differential cross-section.

The design of the detector to measure the μ - e elastic differential cross-section is still under development. There are however some established facts about the possible method and detection technique to be adopted. In order to span most of the Mandelstam's

variable t interval for measuring $\Delta\alpha_{had}(t)$, the experiment has to access high values of the transferred momentum $t = q^2$. As said, the muon energy must be of the order of 150 GeV, in this way it will be possible to achieve for the transferred momentum the value $t = -0.143 \text{ GeV}^2$ going beyond the peak the function represented in figure 2.1, which corresponds to $t \sim -0.108 \text{ GeV}^2$. Namely, to optimally determine a_μ^{HLO} it is crucial reaching values of t that allows to reveal the peak of the integrand function (see figure 2.1). In this respect the high-energy CERN muon beam M2 seems to be an ideal facility. The beam line provides muons in the required energy range and with a high-intensity, of the order of 10^7 muon/s or greater. From the other side, the electron targets have to be made of low Z material, like for instance Beryllium or Carbon. Low Z allows to minimise the effects on the scattered particles of the multiple scattering and the energy loss due to ionization and radiative processes.

The whole target's thickness has to provide the required luminosity. It can be estimated by requiring a statistical precision to measure the cross-section of the order of 10 ppm. The size of the data sample must be of the order of 10^{12} events. The angular distribution of the elastic scattered electrons according to the leading order scattering cross-section is shown in Figure 2.6.

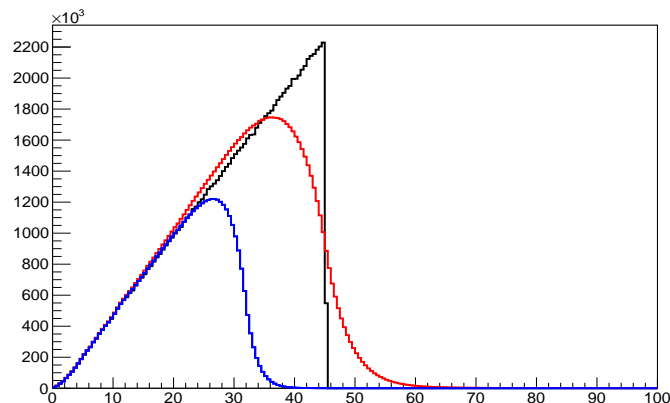


Figure 2.6: In black distribution of the electron scattering angles according to the leading order $\mu - e$ elastic cross section (Monte Carlo limited to about 45mrad). In red the observable distribution. In blue the observed distribution for electron energy greater than 1 GeV.

The histogram in black represents the distribution of 10^8 Monte Carlo simulated events, according to the elastic differential cross-section, while the histogram in red represents the observable electron angular distribution. In blue the observable angles requiring an electron energy above 1 GeV. The target, in this examples, is assumed to be of Beryllium of a thickness of 30 mm. One can notice that most of the events are

produced at relatively small energy with large electron angles. The informative part of the spectrum, where the running of α is appreciable, is below 20 mrad.

The instantaneous luminosity can be calculated as:

$$\mathcal{L} = I_\mu \times \rho_e \times d = I_\mu \times \frac{N_A \cdot \rho \cdot Z}{W} \times d \quad (2.39)$$

where I_μ is the intensity of the muon beam, ρ_e is the density of the electron scattering centers and d is the thickness of the target. ρ_e in turn can be expressed in terms of the material density ρ , the Avogadro's number N_A , the atomic number Z and the atomic weight W .

Assuming the intensity of the muon beam to be $I_\mu = 1.3 \times 10^7 \text{ s}^{-1}$, the luminosity provided by Beryllium target, with $\rho_{Be} = 1.85 \text{ gcm}^3$, $(Z/W)_{Be} = 0.44$, and a thickness $d = 60 \text{ cm}$ is:

$$\mathcal{L}_{Be} = 3.9 \times 10^{32} \text{ cm}^{-2}\text{s}^{-1} = 0.39 \text{ nb}^{-1}\text{s}^{-1} \quad (2.40)$$

The required luminosity that can be collected in two years of data taking, assuming $2 \times 10^7 \text{ s/yr}$ is:

$$L_{Be} = 1.5 \times 10^7 \text{ nb}^{-1} \quad (2.41)$$

Assuming the muon electron elastic scattering cross-section, for scattered electrons of energy greater than 1 GeV is $\sigma_{\mu-e} = 245 \text{ } \mu\text{b}$, then the expected event yield can be estimated to be:

$$N = L_{Be} \times \sigma_{\mu-e} \sim 4 \times 10^{12} \quad (2.42)$$

To detect both the scattered electrons and muons the target overall material budget must be segmented in thin layers, whose thickness have to be optimized in order to limit the effects of the multiple scattering and radiative processes. To optimize the target's thickness one has to estimate the effect of the multiple scattering (MSC) on the observed angular distributions. At the moment the MSC effect can be evaluated only relying on Geant4 Monte Carlo based simulation. The plan is to use thin target of the order of the order of 10 mm.

The differential cross-section will be measured as a function of the electron scattering angles, by revealing event by event both the muon and the electron scattering angles with respect to the direction of the muon beam. The expected analytics relation between the muon and electron angle in the case of elastic scattering for colliding muons of 150 GeV is shown in Figure 2.7. This represents the signature of signal events in the case of elastic scattering.

The layout of the possible detector is sketched in Figure 2.8. The detector is a modular system, consisting of several identical copies of the same module. Each detector module will act as an independent unit. It is equipped with an optimized thin target and with three tracking stations made of Silicon strips. Each Silicon tracking station provides the hit coordinates in the transverse plane. The direction of the particles can be defined tracking the trajectories along the module where the collision occurred.

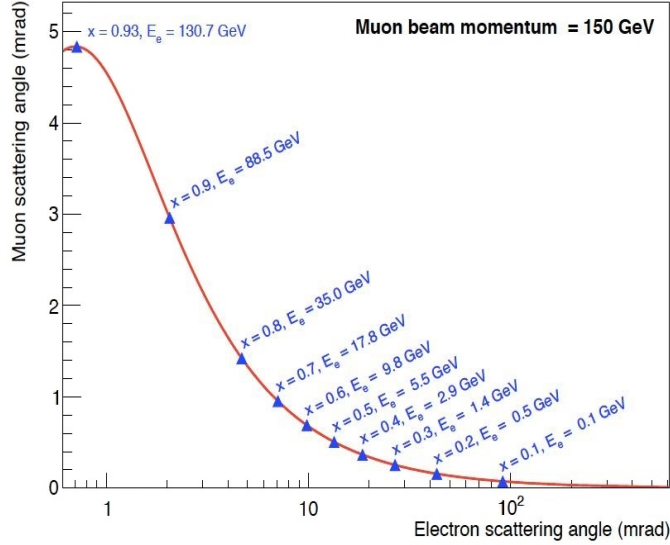


Figure 2.7: The angular correlation of the muon and electron angles in the case of elastic scattering.

The measurement of the differential angular cross-section require a calibration curve, which relates the observed electron angular spectra to the true electron scattering angle distribution. The calibration curve can be determined with the last module of the detector. On this purpose the last module must be equipped with a high-resolution electromagnetic calorimeter. By measuring both the electron angle and the electron energy is it possible to determine the relation between the observed angle and the truth, since the electron energy is in one-to-one relation with the scattering angle. Since all the detector modules are supposed to be identical by construction the calibration curve is the same for all of them.

Evaluating with the best accuracy and precision the effect of MSC is a crucial aspect of the proposed experimental method. Unfortunately, there are not available experimental MSC data to check the prediction of Geant4 about the distortion of the angular distribution we would have in our conditions. We will need therefore to calibrate Geant4 with dedicated measurements of MSC effects, by using electron beams of energetic electrons in the GeV range and Beryllium and Carbon targets of various thickness.

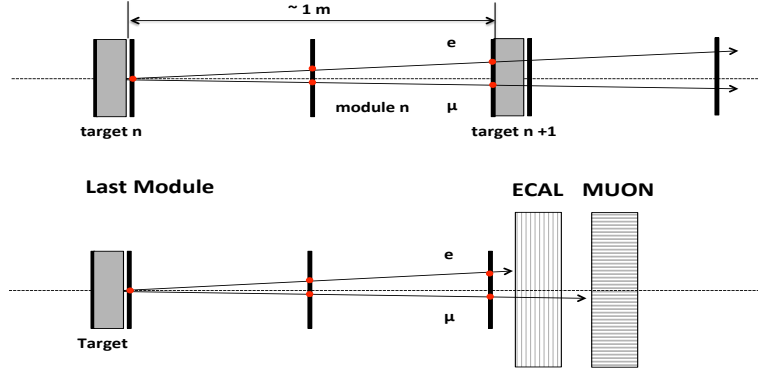


Figure 2.8: The layout of the possible detector to measure the elastic differential cross-section $\mu + e-(rest) \rightarrow \mu + e^-$. It is a modular system, consisting of identical detectors, each made of a thin target and three Silicon strip tracking stations. The last module is equipped with an electromagnetic calorimeter and a muon filter.

2.3 μ - e fitting process

In this paragraph we collect the results of the study performed to determine the statistical precision achievable fitting the $\Delta\alpha(t)$ simulated data. We have used data generated with the Jegerlehner's routine `hadr5n12` [30] [49]. The routine determine the $\Delta\alpha_{had}$ with uncertainty corresponding to the present precision available, obtained with the time-like approach.

We have assumed that the cross-section will be measured as a function of the electron scattering angle θ_e . The cross-section in the electron angle variable can be determined as in the following. Starting from eq. (2.35) and performing a change of variable we get:

$$\frac{d\sigma}{d\theta_e} = \frac{d\sigma}{dt} \left| \frac{dt}{d\theta_e} \right| \quad (2.43)$$

To get the relation between the variable t and the outgoing electron scattering angle we have to determine the energy of the scattered electron $E'_e = E'_e(\theta_e)$. Starting from the squared four-momentum conservation law:

$$(q + p - p')^2 = q'^2 \quad (2.44)$$

which can be written as

$$m_e^2 + p \cdot q - q \cdot p' - p \cdot p' = 0 \quad (2.45)$$

Assuming the components of the four-momenta are the following

$$\begin{aligned}
p &= (m_e, 0, 0, 0) \\
q &= (E_\mu, q, 0, 0) \\
p' &= (E'_e, p' \cos \theta_e, -p' \sin \theta_e, 0) \\
q' &= (E_\mu + m_e - E'_e, q - p' \cos \theta_e, p' \sin \theta_e, 0)
\end{aligned} \tag{2.46}$$

Thereby the four-momenta products are

$$m_e^2 + m_e E_\mu - E_\mu E'_e + qp' \cos \theta_e - m_e E'_e = 0 \tag{2.47}$$

reminding that q and p' are here the modulus of the incoming muon and outgoing electron four-momentum, respectively. Making use of the mass-shell relation for the outgoing electron, we have:

$$q \sqrt{E_e'^2 - m_e^2} \cos \theta_e = (E'_e - m_e) (E_\mu m_e) \tag{2.48}$$

simplifying and taking the square relation:

$$q^2 \cos^2 \theta_e (E'_e - m_e) (E'_e + m_e) = (E'_e - m_e)^2 (E_\mu m_e)^2 \tag{2.49}$$

solving the previous equation:

$$E'_e = m_e \frac{(E_\mu + m_e)^2 + q^2 \cos^2 \theta_e}{(E_\mu + m_e)^2 - q^2 \cos^2 \theta_e} \tag{2.50}$$

Finally, defining

$$r = \frac{\sqrt{E_\mu^2 - m_\mu^2}}{E_\mu + m_e} \tag{2.51}$$

and using the mass-shell relation for the incoming muon, we gain:

$$E'_e = m_e \frac{1 + r^2 \cos^2 \theta_e}{1 - r^2 \cos^2 \theta_e} \tag{2.52}$$

Thus, the relation between the transferred momentum and the electron scattering angle is:

$$\begin{aligned}
t &= 2m_e^2 - 2m_e E'_e \\
&= 2m_e^2 \left(1 - \frac{1 + r^2 \cos^2 \theta_e}{1 - r^2 \cos^2 \theta_e} \right) \\
&= \frac{4m_e^2 r^2 \cos^2 \theta_e}{r^2 \cos^2 \theta_e - 1}
\end{aligned} \tag{2.53}$$

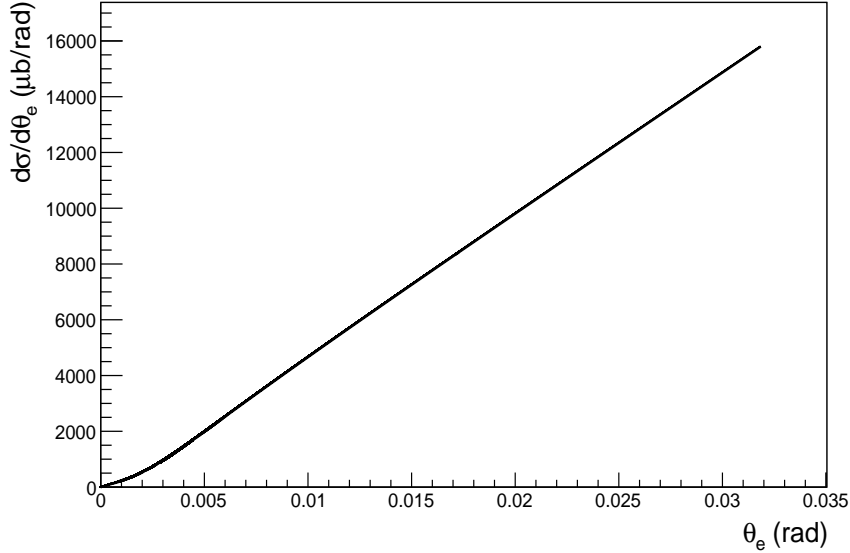


Figure 2.9: The cross-section of μ - e scattering in terms of the electron scattering angle.

At last, we obtain the μ - e scattering differential cross-section in the muon scattering angle:

$$\frac{d\sigma}{d\theta_e} = \frac{8m_e^2 r^2 \cos \theta_e \sin \theta_e}{(r^2 \cos^2 \theta_e - 1)^2} \frac{d\sigma}{dt} \quad (2.54)$$

which is represented in figure 2.9.

The measuring of a differential cross-section is a counting experiment. The quantity $d\sigma/d\theta_e$ will be measured for different values of the electron scattering angle. Let's assume that the range of the possible values of the outgoing electron angle will be split into thirty bins, which will not necessarily of constant width. It might happen that the assumed density of the bins won't be uniform, with higher concentration of counts in the lower θ_e angle limit.

As a first attempt we have supposed to directly measure the μ - e scattering cross-section in the variable t with equidistant bins. Although, this is not a restrictive supposition, it considerably simplifies the fitting procedure. Hence, starting from thirty value with respective error of $d\sigma/dt$, using the Jegerlehner's routine `hadr5n12`, we will calculate thirty values of the function $\Delta\alpha_{had}(t)$ to be fitted.

The mathematical literature suggests that the best class of fitting curves are a Padé approximant, or a third grade polynomial, with null known-term, both of them with

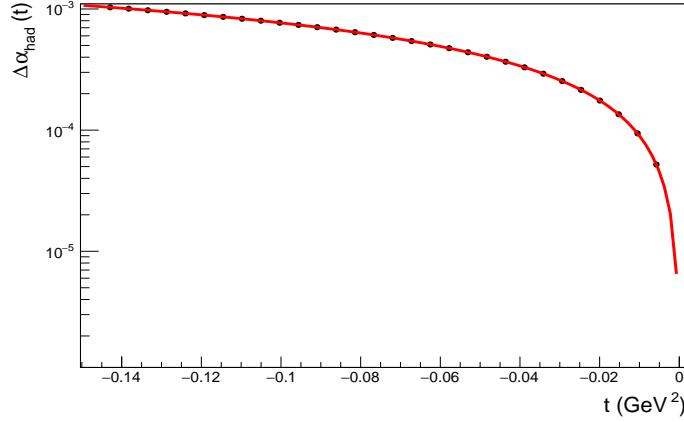


Figure 2.10: The fitting of the thirty equidistant points of $\Delta\alpha_{had}(t)$ with the Padé approximant.

three free parameters [63]:

$$\Delta\alpha_{had}(t) = At \frac{1 + Bt}{1 + Ct} \quad (2.55a)$$

$$\Delta\alpha_{had}(t) = Dt + Et^2 + Ft^3 \quad (2.55b)$$

The Padé approximant, in eq. (2.55a), precisely describe the trend of $\Delta\alpha_{had}(t)$ over the whole t variable interval. On the contrary, the third grade polynomial, eq. (2.55b), approximates $\Delta\alpha_{had}(t)$ only for small values of the Mandelstam's variable, because it comes to infinity when $t \rightarrow \infty$.

The result of the fitting procedure performed with the Padé approximant is shown in figure 2.10. Furthermore, we tried also to perform the fit with the function that describes the leptonic running of α , when the transferred momentum is negative [62], using two fit parameters:

$$\begin{aligned} \Delta\alpha_{had}(t) = & G \left(-\frac{5}{9} - \frac{4H}{3t} + \left(\frac{4H^2}{3t^2} + \frac{H}{3t} - \frac{1}{6} \right) \right. \\ & \left. \times \frac{2}{\sqrt{1 - 4H^2/t}} \ln \left| \frac{1 - \sqrt{1 - 4H^2/t}}{1 + \sqrt{1 - 4H^2/t}} \right| \right) \end{aligned} \quad (2.56)$$

where the coefficient H represents the square of the particles masses that are involved in the process, thus in our case it represents the square of the light quarks masses. While the coefficient G collects many different constants: for instance the color number and the charge of the light quarks. From here to the rest of the thesis we will refer to this curve as the leptonic-like one.

curve	parameter	value
Padé	A	$(-915.15 \pm 3.94) \times 10^{-5}$
	B	-0.680 ± 0.583
	C	-2.728 ± 0.744
polynomial	D	$(-913.83 \pm 3.48) \times 10^{-5}$
	E	$(-17.66 \pm 1.04) \times 10^{-3}$
	F	$(-30.16 \pm 7.03) \times 10^{-3}$
leptonic	G	$(71.93 \pm 1.14) \times 10^{-4}$
	H	$(524.19 \pm 9.34) \times 10^{-4}$

Table 2.1: The fitting parameters obtained by ROOT in the Padé, polynomial and so called leptonic case.

Using the program ROOT [61] to fit the Jegerlener data we obtained the fitting parameters showing in the table 2.1. Note that when fitting with three free parameters as in the case of Padé and polynomial functional form the error associated to one of the parameters is very large. To prove that the error given by ROOT to that parameter, B in Padé case and F in the polynomial case, is well estimated, these parameters have been varied within one standard deviation. The result is that significant deviations were not observed, hence it may could mean that one parameter of them is redundant. On the contrary, the third curve presents small errors, but the open question is to understand why unexpectedly it works.

Once the fitting curves has been obtained, it is necessary to operate a change of variable to get its analytic expression in the x variables, to then solve numerically the integral of eq. (2.8). We remind that the transferred momentum and the variable x are connected by eq. (2.2).

We numerically integrated the three curves in the range $0 \leq x \leq 0.93212$, where the upper limit corresponds to the lower limit of the t variable, which is equals to -0.142893 due to the the value of the muon beam energy set to 150 GeV. The numerical integration has been performed by means ROOT, using the already available Gaussian method [64]. The results of the previous integration methods are in close agreement, thus we report the only Gaussian one:

$$\begin{aligned}
 I_{Pad} &= 600.837 \times 10^{-10} \\
 I_{pol} &= 600.671 \times 10^{-10} \\
 I_{lep} &= 600.771 \times 10^{-10}
 \end{aligned}$$

The ratio between the integrations done over $0 \leq x \leq 0.93212$ and over the full range of the x variable, is equal to the 87.2%. Thus we have to compare the previous results

with the that obtained with Jegerlehner's routine, which is quite different from his last value presentad above in eq. (1.114):

$$[65] \quad I_{Jeg} = (600.75 \pm 4.28) \times 10^{-10} \quad (2.57)$$

The goal of this thesis is to associate a statistical uncertainty to the 87.2% of the full integral. To achieve it, we have simulated, with a ROOT program which uses a cycle, one million events. The fitting procedure, explained above, has been repeated for each iteration: the program extracts from the Jegerlehner routine the thirty value of $\Delta\alpha_{had}$ and gaussian varies each one of them with standard deviation equals to error associated to that value. Then the fitting parameters of the three curves have been calculated to obtain the approximated analytical function of $\Delta\alpha_{had}(t)$. Changing the variable, from t to x , and integrate it over the usual range $0 \leq x \leq 0.93212$, we have obtained, for each iteration, the value of the 87.2% of the hadronic leading-order contribution to a_μ . We have applied this recipe for all the three curves.

Performing a statistical analysis on the one million data, we have:

$$\begin{aligned} I_{Pad} &= (600.15 \pm 1.24) \times 10^{-10} \\ I_{pol} &= (600.67 \pm 1.21) \times 10^{-10} \\ I_{lep} &= (600.77 \pm 1.14) \times 10^{-10} \end{aligned} \quad (2.58)$$

The error associated to each integral, of about 0.2%. It is obtained by a purely statistical consideration, although it is both statistical and systematic: the $\Delta\alpha_{had}$ error given by the Jegerlehner's routine is already a combination between the statistical and systematics uncertainty. We have done this calculation only to test our fitting procedure. Now, we have to repeat the procedure but after associating the statistical error related to the μ - e scattering process.

2.4 Computation of the $\Delta\alpha_{had}(t)$ absolute error

As last step, we have calculated the the error associated to each one of the thirty values of $\Delta\alpha_{had}(t)$, still keeping the hypothesis of measuring the μ - e cross-section with respect to the t variable. Starting from eq. (2.37) and using the error dispersion rules, we have:

$$\delta\sigma = 2 \frac{\alpha_0^2}{(1 - \Delta\alpha(t))^3} \frac{d\sigma_0}{dt} \delta\Delta\alpha(t) \sim 2\sigma\delta\Delta\alpha(t) \quad (2.59)$$

Recalling eq. (2.10), we get

$$\delta\sigma = 2\sigma\delta\Delta\alpha_{had}(t) \quad (2.60)$$

The previous equation can be written as

$$\Delta\alpha_{had} = \frac{1}{2} \frac{\delta\sigma}{\sigma} \quad (2.61)$$

Measuring the μ - e cross-section means counting the event rate (R_i) of each bin:

$$R_i = \frac{dN_i}{dt} = \sigma_i \cdot L \quad (2.62)$$

where L is the luminosity and σ_i is the cross-section of a particular bin. The index i runs from one to thirty, in the hypothesized case. From eq. (2.62) we get that the ratio relative error (δR_i) is equal to the cross-section relative error ($\delta \sigma_i$).

Because of the error in a counting experiment is equal to the square root of the counts, we have:

$$\Delta \alpha_{had,i} = \frac{1}{2} \frac{\delta \sigma_i}{\sigma_i} = \frac{1}{2} \frac{\delta R_i}{R_i} = \frac{1}{2} \frac{1}{\sqrt{\sigma_i \cdot L}} \quad (2.63)$$

we immediately notice that, because of the increasing monotonic behavior of the cross-section with respect the transferred momentum, the error associated to each bin decreases in the limit $t \rightarrow 0$.

In the limit of narrow bins we have:

$$\begin{aligned} \delta \Delta \alpha_{had,i} &= \frac{1}{2} \frac{1}{\sqrt{\frac{d\sigma_i}{dt} \Delta t L}} \\ &= \frac{1}{2} \frac{1}{\sqrt{\int_{bin_i} \frac{d\sigma_i}{dt} dt L}} \end{aligned} \quad (2.64)$$

The lower limit of the transferred momentum is equal to $t_{low} = -0.142893 \text{ GeV}^2$, while the upper limit, obtained cutting the scattered electron energy at 1 GeV, is $t_{up} = -0.00102148 \text{ GeV}^2$. Dividing the whole t range in thirty equidistant bins, the bin width is $\Delta t = 0.00472907 \text{ GeV}^2$. Taking as an example the last bin with $-0.00574997 < t < -0.0010209$, we obtain for cross-section $\sigma_{30} = 0.206788 \text{ mb}$ and thereby, from eq. (2.64), with a luminosity of $L = 1.5 \cdot 10^7 \text{ nb}^{-1}$, we obtain:

$$\delta \Delta \alpha_{had,30} = 2.83 \cdot 10^{-7} \quad (2.65)$$

In figure 2.11 has been represented all the $\delta \Delta \alpha_{had,i}$ absolute error as points at the middle of the corresponding bin, although $\Delta \alpha_{had}(t)$ must be a step function.

The goal of this thesis is to associate a statistical error to the measurable hadronic leading-order contribution, 87.2% of to the anomalous magnetic moment. Repeating the above procedure using one million simulated measurements, with our estimated uncertainties on the thirty values of $\Delta \alpha_{had}(t)$, instead of those given by Jegerlehner's routine. With our uncertainties, we get:

$$\begin{aligned} I_{Pad} &= (600.81 \pm 1.67) \times 10^{-10} \\ I_{pol} &= (600.82 \pm 1.67) \times 10^{-10} \\ I_{lep} &= (600.81 \pm 1.67) \times 10^{-10} \end{aligned} \quad (2.66)$$

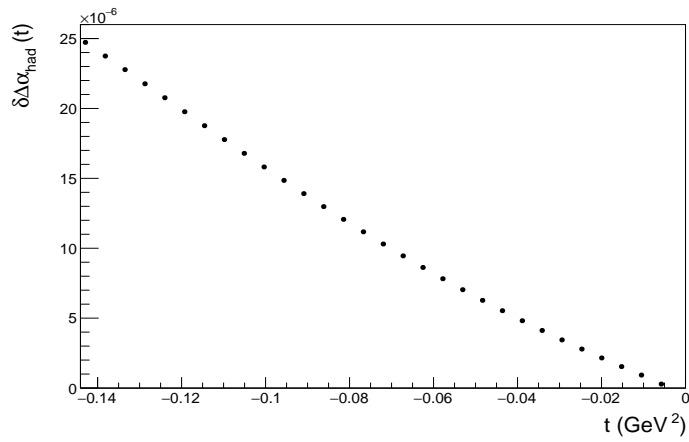


Figure 2.11: The $\Delta\alpha_{had}(t)$ absolute error with respect to the transferred momentum.

The associated error, statistically calculated, is about 0.3%. To obtain the complete error of the hadronic leading-order contribution, one must adding up the systematic error, however it is not already available.

Appendix A

Feynman Parameters

R. Feynman developed a method to simplify the integration procedure of a rational integrand function, whose denominator can be written as a product of polynomial functions. The goal of this method is to squeeze the denominators of an integrand function into a single polynomial, making use of variables called *Feynman parameters* [7]

$$\frac{1}{A_1 \dots A_n} = \int_0^1 dx_1 \dots dx_n \delta \left(1 - \sum_{i=1}^n x_i \right) \frac{(n-1)!}{[x_1 A_1 + \dots + x_n A_n]^n} \quad (\text{A.1})$$

The most general Feynman parametric formula is

$$\begin{aligned} \frac{1}{A_1^{a_1} \dots A_n^{a_n}} &= \frac{\Gamma(a_1 + \dots + a_n)}{\Gamma(a_1) \dots \Gamma(a_n)} \times \int_0^1 dx_1 \dots \int_0^1 dx_n \delta \left(1 - \sum_{i=1}^n x_i \right) \\ &\quad \times (x_1^{a_1-1} \dots x_n^{a_n-1}) (x_1 A_1 + \dots + x_n A_n)^{-a_1 - \dots - a_n} \end{aligned}$$

A.1 One-loop integrals

It is useful to define

$$\int_p = \mu^{4-2\omega} \int \frac{d^{2\omega} p}{(2\pi)^{2\omega}}$$

where μ is an arbitrary mass scale, introduced with a suitable exponent, in such a manner to deal with a dimensionless of the integral. Moreover [9]

$$\begin{aligned} I(a, b) &= \int_p \frac{1}{(p^2 - \Delta^2 + i\varepsilon)^a [(p-l)^2 - \Delta^2 + i\varepsilon]^b} \\ I^\mu(a, b) &= \int_p \frac{p^\mu}{(p^2 - \Delta^2 + i\varepsilon)^a [(p-l)^2 - \Delta^2 + i\varepsilon]^b} \\ I^{\mu\nu}(a, b) &= \int_p \frac{p^\mu p^\nu}{(p^2 - \Delta^2 + i\varepsilon)^a [(p-l)^2 - \Delta^2 + i\varepsilon]^b} \end{aligned}$$

In the case of interest $a = 3$ and $b = 0$. In the scalar case the integral gives:

$$\lim_{\omega \rightarrow 2} I(3, 0) = \frac{-i}{32\pi^2} \frac{1}{(-\Delta^2 + i\varepsilon)^a} \quad (\text{A.2})$$

and in the two rank tensor case

$$I_{\mu\nu}(3, 0) = \frac{-i}{16\pi^2} g_{\mu\nu} \frac{\Gamma(2 - \omega)}{8} (4\pi\mu^2)^{2-\omega} \frac{1}{(-\Delta^2 + i\varepsilon)^a} \quad (\text{A.3})$$

Appendix B

Gordon Identities

Starting from:

$$\gamma^\mu \not{q} = \frac{1}{2} (\{\gamma^\mu; \not{q}\} + [\gamma^\mu; \not{q}]) = \frac{1}{2} q_\nu 2g^{\mu\nu} + \frac{1}{2} (-4iq_\nu \sigma^{\mu\nu}) = q^\mu - 2i\sigma^{\mu\nu} q_\nu \quad (\text{B.1a})$$

$$\not{p} \gamma^\mu = \frac{1}{2} (\{\gamma^\mu; \not{p}\} + [\gamma^\mu; \not{p}]) = \frac{1}{2} p_\nu 2g^{\mu\nu} - \frac{1}{2} (-4ip_\nu \sigma^{\mu\nu}) = p^\mu - 2i\sigma^{\mu\nu} p_\nu \quad (\text{B.1b})$$

the results are due to the algebra of γ -matrices in the usual four dimensions space, namely:

$$\begin{aligned} \{\gamma^\mu; \gamma^\nu\} &= 2g^{\mu\nu} \mathbb{1}_{4 \times 4} \\ [\gamma^\mu; \gamma^\nu] &= -4i\sigma^{\mu\nu} \end{aligned}$$

Therefore it is possible to write:

$$q^\mu - 2i\sigma^{\mu\nu} q_\nu = m\gamma^\mu + \gamma^\mu (\not{q} - m) \quad (\text{B.2a})$$

$$p^\mu + 2i\sigma^{\mu\nu} q_\nu = m\gamma^\mu + (\not{p} - m) \gamma^\mu \quad (\text{B.2b})$$

where as usual $\sigma^{\mu\nu} = \frac{i}{4} [\gamma^\mu; \gamma^\nu]$. Moreover we obtain:

$$\begin{aligned} \not{q} \gamma^\mu \not{p} &\doteq (\not{k} + \not{p}) \gamma^\mu (\not{q} - \not{k}) \\ &= (\not{k} + m) \gamma^\mu (m - \not{k}) \\ &= m^2 \gamma^\mu - \not{k} \gamma^\mu \not{k} - m [\gamma^\mu; \not{k}] \\ &= m^2 \gamma^\mu - k_\alpha k_\beta \gamma^\alpha \gamma^\mu \gamma^\beta - m k_\alpha [\gamma^\mu; \gamma^\alpha] \\ &= m^2 \gamma^\mu - k_\alpha k_\beta (\gamma^\alpha \{\gamma^\mu; \gamma^\beta\} - \gamma^\alpha \gamma^\beta \gamma^\mu) + 4im\sigma^{\mu\alpha} k_\alpha \\ &= m^2 \gamma^\mu - 2\not{k} k^\mu + \not{k} \not{k} \gamma^\mu + 4im\sigma^{\mu\alpha} k_\alpha \\ &= m^2 \gamma^\mu + \not{k}^2 \gamma^\mu + 4im\sigma^{\mu\alpha} k_\alpha \end{aligned} \quad (\text{B.3})$$

where the symbol \doteq means that we are applying spin states $\bar{u}(q)(\dots)u(p)$ and the Dirac equation is valid and also the mass-shell relations. In the very last step we used $\not{k} =$

$\not{q} - \not{p} \doteq 0$.

Finally, Gordon identities read:

$$\not{q}\gamma^\mu = [\not{q}; \gamma^\mu] + \gamma^\mu \not{q} \doteq 4i\sigma^{\mu\alpha} q_\alpha + m\gamma^\alpha \quad (\text{B.4a})$$

$$\gamma^\mu \not{p} = [\gamma^\mu; \not{p}] + \not{p}\gamma^\mu \doteq -4i\sigma^{\mu\alpha} p_\alpha + m\gamma^\alpha \quad (\text{B.4b})$$

Appendix C

Traces of Dirac matrices

Is necessary to make a distinction between a trace of an even or an odd number of Dirac matrices.

The trace of an odd number of Dirac matrices is always zero. On the contrary, for an even number of them we have to calculate the result. We now compute the trace of two and four Dirac matrices, enough for the calculations in the thesis.

1. **Trace of two Dirac matrices** The trick that we will use to solve the trace is to rewrite the product of Dirac matrices as a sum of commutators and anti-commutators. Moreover, due to the cyclic nature of the trace, we know that the trace of any commutator is null. Thus we have:

$$\begin{aligned}\mathrm{tr}(\gamma^\mu\gamma^\nu) &= \mathrm{tr}\left(\frac{1}{2}\{\gamma^\mu;\gamma^\nu\} + \frac{1}{2}[\gamma^\mu;\gamma^\nu]\right) \\ &= \frac{1}{2}\mathrm{tr}(\{\gamma^\mu;\gamma^\nu\}) + \frac{1}{2}\mathrm{tr}([\gamma^\mu;\gamma^\nu]) \\ &= \frac{1}{2}\mathrm{tr}(\{\gamma^\mu;\gamma^\nu\}) \\ &= \frac{1}{2}\mathrm{tr}(2g^{\mu\nu}\mathbb{1}_{4\times 4}) \\ &= 4g^{\mu\nu}\end{aligned}\tag{C.1}$$

2. **Trace of four Dirac matrices** The trick to solve the trace of four Dirac is quite different from that we used in the previous item: we have to cycle two matrices

a times

$$\begin{aligned}
\text{tr}(\gamma^\mu \gamma^\nu \gamma^\rho \gamma^\sigma) &= \text{tr}(\gamma^\mu \gamma^\nu \gamma^\rho \gamma^\sigma + \gamma^\nu \gamma^\mu \gamma^\rho \gamma^\sigma - \gamma^\nu \gamma^\mu \gamma^\rho \gamma^\sigma) \\
&= \text{tr}(\{\gamma^\mu; \gamma^\nu\} \gamma^\rho \gamma^\sigma - \gamma^\nu \gamma^\mu \gamma^\rho \gamma^\sigma) \\
&= \text{tr}(2g^{\mu\nu} \gamma^\rho \gamma^\sigma - \gamma^\nu \gamma^\mu \gamma^\rho \gamma^\sigma) \\
&= 2g^{\mu\nu} \text{tr}(\gamma^\rho \gamma^\sigma) - \text{tr}(\gamma^\nu \gamma^\mu \gamma^\rho \gamma^\sigma + \gamma^\nu \gamma^\rho \gamma^\mu \gamma^\sigma - \gamma^\nu \gamma^\rho \gamma^\mu \gamma^\sigma) \\
&= 8g^{\mu\nu} g^{\rho\sigma} - 2g^{\mu\rho} \text{tr}(\gamma^\nu \gamma^\sigma) + \text{tr}(\gamma^\nu \gamma^\rho \gamma^\mu \gamma^\sigma) \\
&= 8g^{\mu\nu} g^{\rho\sigma} - 8g^{\mu\rho} g^{\nu\sigma} + \text{tr}(\gamma^\nu \gamma^\rho \gamma^\mu \gamma^\sigma + \gamma^\nu \gamma^\rho \gamma^\sigma \gamma^\mu - \gamma^\nu \gamma^\rho \gamma^\sigma \gamma^\mu) \\
&= 8g^{\mu\nu} g^{\rho\sigma} - 8g^{\mu\rho} g^{\nu\sigma} + 8g^{\nu\rho} g^{\mu\sigma} - \text{tr}(\gamma^\nu \gamma^\rho \gamma^\sigma \gamma^\sigma \mu)
\end{aligned} \tag{C.2}$$

using the property of cyclicity in the last term of the previous equation, we finally obtain:

$$\text{tr}(\gamma^\mu \gamma^\nu \gamma^\rho \gamma^\sigma) = 4(g^{\mu\nu} g^{\rho\sigma} - g^{\mu\rho} g^{\nu\sigma} + g^{\nu\rho} g^{\mu\sigma}) \tag{C.3}$$

Conclusion

Muon anomaly represents a fascinating subject. Precise theoretical predictions compared to the experimental results could enable researchers to reveal possible failures of the Standard Model (SM).

The present discrepancy between SM predictions and experimental result is at the level of $\sim 3.8\sigma$. It is considered amongst the others an important tension of the Standard Model. It is not however large enough to unambiguously indicate the need of new physics, claiming for new contributions beyond the SM.

Theoretical calculations and experiments have to reach higher precisions. Plans to improve the current precisions in the next years both theoretically and experimentally have been proposed. From the experimental side, there are two major experiments presently under construction, at Fermilab and JPARK, aiming to improve the precision on the muon anomaly by a factor four. It will be highly desirable for that time to get a SM prediction of improved precision too. It implies reaching of a greater precision on the determination of the leading hadronic contribution to muon anomaly, the major source of the present theoretical uncertainty.

In this thesis I have discussed a novel approach to evaluate the leading hadronic contribution, based on the measurement of the running of the fine-structure constant α as a function of space-like transferred momentum, to be determined by means of the elastic scattering of high-energy muons colliding on electrons at rest. I have proved that by using a muon beam of 150 GeV, with an intensity of the order of 10^7 muon/s, and assuming two years of data taking, the proposed new experiment could allow to determine the leading hadronic contribution with a statistical uncertainty of 0.3%. Provided that systematic uncertainty will be kept at the same level the precision would be competitive with the precision achievable with the standard method, which has been obtained with many different experiments relying on the dispersive approach exploiting e^+e^- annihilation time-like data.

This new experimental method could provide an important result to improve the Standard Model predictions.

Measurements of the muon anomaly with the planned high-precision can be used in conjunction with future collider results, at the energy frontier, to reveal possible signs of new physics, and constrain further possible theoretical development beyond the SM.

Ringraziamenti

Queste ultime righe sono dedicate a coloro che mi hanno aiutato e incoraggiato in questo percorso.

Ringrazio il prof. Domenico Galli, relatore della tesi, per la disponibilità e cortesia dimostrate, e per l'aiuto fornito durante la stesura. Ringrazio i correlatori: il dott. Carlo M. C. Calame per avermi guidato costantemente nel lavoro di tesi, mostrando una inossidabile pazienza, e il dott. Massimo Passera, per i suoi fondamentali insegnamenti teorici e per aver stimolato il mio interesse verso questo innovativo progetto.

Al dott. Umberto Marconi, già correlatore in triennale, per avermi nuovamente coinvolto nei suoi studi; maestro, non solo di questa nobile scienza, ma anche di vita, a lui rivolgo un ringraziamento particolare.

Proseguo ringraziando Alvaro e Cinzia, il loro incessante sostegno e incoraggiamento hanno permesso il raggiungimento di questo obiettivo. Grazie papà e mamma. Ringrazio Alessandra, mia sorella, per essere presente in ogni istante.

Desidero poi ringraziare i miei amici, quelli "*dei giardini*", che ci sono incondizionatamente. Da sempre. Grazie ragazzi.

Un ringraziamento va agli amici di Bologna, conosciuti sui banchi di una vecchia aula magna, con i quali ho condiviso non solo interminabili ore di lezione e monumentali esami, ma soprattutto bellissime serate in questa città. Ringrazio gli amici di Padova che, con filosofiche riflessioni sulla vita e piacevoli post-cena, hanno colorato questi faticosi mesi di tesi.

Un ringraziamento particolare va infine ai miei coinquilini bolognesi: a Filippo, con il quale ho iniziato questa avventura, per gli indimenticabili disastri combinati insieme; a Marco e Paolo, con i quali l'ho conclusa, per gli istruttivi confronti, le agguerrite partite a carte e le interminabili discussioni notturne.

Bibliography

- [1] Eisberg R., Resnick R., Quantum Physics, Wiley, 2014.
- [2] Bransden B. H., Joachain C. J., Physics of Atoms and Molecules, Pearson, 2014.
- [3] AA. VV., "Particle Data Group", <http://pdg.lbl.gov/2017/listings/rpp2017-list-electron.pdf>, 2017.
- [4] Passera M. 2005 *J. Phys. G* **31** R75.
- [5] Itzykson C. and Zuber J. B., Quantum Field Theory, Dover Publications, 2005.
- [6] Soldati R., Advances in Quantum Field Theory, Bologna, 2016.
- [7] Peskin M., Schroeder D., An Introduction to Quantum Field Theory, Westview Press, 2016.
- [8] Jegerlehner F., The Anomalous Magnetic Moment of the Muon, Berlino, 2007.
- [9] Soldati R., Intermediate Quantum Field Theory, Bologna, 2016.
- [10] Elend H. H. 1966 *Phys. Lett.* **20** 682.
- [11] Passera M. 2007 *Phys. Rev. D* **75** 013002.
- [12] Mhor P. J. and Taylor B. N. 2005 CODATA recommended values of the fundamental physical constants: 2002 *Rev.*
- [13] Aoyama T., Hayakawa M., Kinoshita T., Nio M. 2012 *Phys. Rev. Lett.* **109** 111808.
- [14] Kinoshita T., Cvitanovic P. 1972 *Phys. Rev. D* **29** 22.
- [15] Laporta S. and Remiddi E. 1995 *Phys. Lett. B* **356** 390.
- [16] Laporta S. and Remiddi E. 1996 *Phys. Lett. B* **379** 283.
- [17] Laporta S. and Remiddi E. 1993 *Phys. Lett. B* **301** 440.

- [18] Kinoshita T. and Nio M. 2004 *Phys. Rev. D* **70** 113001.
- [19] Kinoshita T. and Nio M. 2006 *Phys. Rev. D* **73** 053007.
- [20] Laporta S. 2017 *Phys. Lett. B* **772** 232-238.
- [21] Czarnecki A., Krause B. and Marciano W. J. 1995 *Phys. Rev. D* **52** 3267.
- [22] AA. VV., "Particle Data Group", <http://pdg.lbl.gov/2017/tables/rpp2017-sum-gauge-higgs-bosons.pdf>, 2017.
- [23] Kukhto T., Kuraev E., Schiller A. and Silagad Z. 1992 *Nucl. Phys. B* **371** 567.
- [24] Gnendiger C., Stöckinger D., Stöckinger-Kim H. 2013 *Phys. Rev. D* **88** 053005.
- [25] Melnikov K., Vainshtein A., Theory of the Muon Anomalous Magnetic Moment, Berlino, 2006.
- [26] VV. AA., "The E821 Muon (g-2) Home Page", <http://www.g-2.bnl.gov/>, 2017.
- [27] Bouchiat C., Michel J., 1962 *Phys. Rev.* **128** 441.
- [28] Passera M., "The muon g-2 recent progress", Padova, 2016.
- [29] Davier D. *et al* 2011 *Preprint EPJ C* **71** 1515.
- [30] Eidelman S. and Jegerlehner F. 1995 *Z. Phys. C* **67** 585.
- [31] Lees J. P. *et al* (BABAR collaboration) 2012 *Phys. Rev. D* **86** 012008.
- [32] Lees J. P. *et al* (BABAR collaboration) 2012 *Phys. Rev. D* **86** 032013.
- [33] Lees J. P. *et al* (BABAR collaboration) 2012 *Phys. Rev. D* **89** 111103.
- [34] Lees J. P. *et al* (BABAR collaboration) 2013 *Phys. Rev. D* **88** 032013.
- [35] Lees J. P. *et al* (BABAR collaboration) 2013 *Phys. Rev. D* **87** 092005.
- [36] Bernard D. 2017 *Nucl. Part. Phys. Proc.* **282-284** 132-138.
- [37] Liu W. *et al.* 1999 *Phys. Rev. Lett.* **82** 711.
- [38] AA. VV., "Particle Data Group", <http://pdg.lbl.gov/2017/listings/rpp2017-list-muon.pdf>, 2017.
- [39] Calame C. M. C., Passera M., Trentadue L., Venanzoni G. 2015 *Phys. Lett. B* **746** 325.

- [40] Abbiendi G. *et al* 2017 *Eur. Phys. J. C* **77** 139.
- [41] Jegerlehner F., Nyffeler A., 2009 *Phys. Rep.* **477** 110.
- [42] Barone V., *Relatività*, Bollati Boringhieri, 2004.
- [43] Schwinger J. 1948 *Phys. Rev.* **73** 416.
- [44] Sommerfield C. M. 1957 *Phys. Rev.* **107** 328.
- [45] Davier M., Marciano W. J. 2004 *Annu. Rev. Nucl. Part. Sci.* 54:115–40.
- [46] Davier M., Eidelman S., Höcker A. and Zang Z. 2003 *Eur. Phys. J. C* **31** 503.
- [47] Akhmetshin R. R. *et al* (CMD-2 Collaboration) 2004 *Phys. Lett. B* **578** 285.
- [48] Jegerlehner F. 2017 *Springer Tracts Mod. Phys.* **274** 1-693.
- [49] Jegerlehner F. 2008 *Nucl. Phys. Proc. Suppl* **181-182** 135.
- [50] Hagiwara K. *et al* 2011 *Preprint* JPG 38 085003.
- [51] Hagiwara K., Martin A. D., Nomura D. and Teubner T. 2002 *Phys. Lett. B* **557** 69-75.
- [52] Chapelain A. 2017 *EPJ Web Conf.* **137** 08001.
- [53] Venanzoni G. 2012 *Phys. Series* Vol. LVI.
- [54] Gray F. 2015 (Muon $g-2$ collaboration) arXiv:1510.00346.
- [55] Anastasi A. 2017 EPJ Web of Conferences **142** 01002.
- [56] Kim S. C. "<https://inspirehep.net/record/1419022/files/fermilab-conf-15-576-ade.pdf>", 2017.
- [57] Davier M. *et al.* 2017 arXiv:1706.09436.
- [58] de Rafael E. 2017 *Phys. Rev. D* **96** 014510.
- [59] Della Morte M. *et al* "The hadronic vacuum polarization contribution to the muon $g - 2$ from lattice QCD", 2017.
- [60] Steinhauser M. 1998 *Nucl. Phys. B* **429** 158.
- [61] VV. AA., "<https://root.cern.ch/>", 2017.
- [62] Calame C. M. C., Tesi di dottorato, Pavia, 2001.

- [63] Baker A. G., Gamme J. L., The Padé Approximant in Theoretical Physics, Academic Press, 1970.
- [64] VV. AA., "<https://root.cern.ch/function-integration>", 2017.
- [65] Calame C.M.C., "Fits for a_{HLO}^μ space-like.", 2017.